IMPROVING THE DIAGNOSIS OF BLOOD STREAM INFECTIONS WITH BECTON DICKINSON'S BACTEC™ AUTOMATED LIQUID CULTURE SYSTEM

by

Shannon Martello

A thesis submitted to Johns Hopkins University in conformity with the requirements for the degree of Master of Science in Engineering in Chemical and Biomolecular Engineering

Baltimore, Maryland
July 2018

ABSTRACT

Sepsis is a highly dynamic condition caused by a dysregulated host response to a pathogen in the bloodstream. Fast and accurate diagnosis of the causative pathogen is critical to provide effective treatment and minimize the risk of death. The current diagnostic workflow for a blood stream infection begins with a blood draw from the patient into a culture bottle, which is then incubated in an automated blood culture instrument to detect growth of the pathogen. Common automated blood culture systems, such as Becton Dickinson's BACTEC franchise, utilize glass culture bottles containing a fluorescence-based sensor to aid detection of bacterial growth. After detection of growth by the instrument, the bacteria are isolated via an overnight subculture to provide a sample for downstream testing. Once isolated, bacteria can then be identified and tested for antimicrobial susceptibility.

In this thesis, we characterize and optimize two aspects of the diagnostic workflow in order to improve sepsis diagnosis and patient management. The first chapter details characterization of and improvements to a filtration system designed to decrease the time to diagnosis by isolating bacteria from a positive blood culture in 15 minutes. To improve the quality of the isolated sample for accurate identification and antimicrobial susceptibility testing, we assessed the current performance of the system. We then improved recovery and downstream results by adjusting the filtration workflow and increasing the area through which the positive blood culture is filtered. The second chapter targets conversion of the current glass blood culture bottle to a safer, lighter polycarbonate bottle. We characterized formulations for the polycarbonate bottle's fluorescence-based sensor in order to ensure proper adhesion to the bottle and define the signal ranges. With this, we selected a formulation for scale up to biological testing, which will assess the sensitivity of signal detection and allow the new polycarbonate bottle to be brought to market. Both

conversion of the blood culture bottle to a safer material and reduction of bacterial isolation time will improve the diagnostic workflow for a bloodstream infection, ultimately allowing for easier diagnosis and treatment of sepsis.

Advisors:

Richard L. Moore, M.D., Ph.D., Becton Dickinson Diagnostic Systems

Professor Rebecca Schulman, Ph.D., Johns Hopkins University

Second Reader:

Professor Chao Wang, Ph.D., Johns Hopkins University

ACKNOWLEDGEMENTS

After five years at Hopkins, there are a countless number of people to whom I owe a great deal of thanks. For guidance and advice related to both academics and my career, I would like to thank my advisor, Dr. Rebecca Schulman. I would also like to thank Tom Fekete and those responsible for the INBT Master's co-op program for providing me with this unique opportunity and being flexible when things at Becton Dickinson did not go according to plan.

The work covered in this thesis would not have been possible without BD. I owe a great deal of gratitude to my supervisor, Dr. Richard Moore, for continuously supporting the many projects I worked on. I cannot express how thankful I am for helping me make things work despite all the road bumps and my sometimes unnecessarily high stress levels. I would also like to thank all of the Microbiology R&D teams I worked with at BD for continued support throughout my entire co-op.

Lastly, I would like to thank my friends and family. These past five years and two degrees were made possible and far more enjoyable thanks to your love and support.

.

TABLE OF CONTENTS

LIST OF TABLES

LIST OF FIGURES

Chapter 1: Optimization of Positive Blood Culture Processing for Rapid Identification and Antimicrobial Susceptibility Testing of Bacteria in Blood Stream Infections

ABSTRACT

Sepsis, clinically defined as a dysregulated host response to a pathogen in the bloodstream, accounts for 25% of hospital deaths and $20 billion in health care expenses annually[1, 2]. Diagnosis of the causative infection requires a blood culture to detect growth of microorganisms, followed by evaluation of the positive blood culture (PBC) for identification (ID) and antimicrobial susceptibility testing (AST). Rapid and accurate ID/AST results are critical to avoid broad or ineffective treatment and minimize toxicity to beneficial bacteria. Current ID/AST workflows require an 18-hour subculture from the PBC to provide an isolated sample for downstream testing. Previous work confirmed the feasibility of using tangential flow filtration to isolate bacteria from a PBC in 15 minutes, reducing the time required for isolation; however, this concept requires further development to reduce processing time, maximize output, and minimize loss of bacteria.

We used the filtration system to process 30 strains of bacteria grown in three different types of BACTEC (Becton Dickinson (BD)) media in order to set a baseline of performance for filtration (PBC processing), matrix-assisted laser desorption/ionization time-of-flight mass spectrometry (MALDI ToF MS) ID, and Phoenix™ (BD) AST. Baseline performance results showed that Gram negative bacteria filter well to yield accurate ID/AST results across all three media types; however, Gram positive bacteria proved difficult to filter and did not consistently yield accurate ID/AST results. We attributed these difficulties to lack of bacteria and excess blood background in the output. In order to provide a more isolated and concentrated sample, we targeted the lysis and wash steps of PBC processing. Furthermore, we hypothesized that lack of bacteria stems from cake layer formation atop the filter membrane, becoming more apparent for smaller filter pore sizes. For Gram positive bacteria, we also attributed lack of bacteria to their clumping nature and subsequent

inability to fit through the pores. Thus, we increased the pore size and yielded higher percent recovery and more accurate ID/AST results for the problematic Gram positive bacteria.

Further optimization of filter geometry, operating vacuum pressure, and sample flowrate will minimize cake formation and improve isolated bacterial recovery. Moreover, definition of limits of detection for MALDI ID and Phoenix AST will set standards for filter performance, allowing for more rapid and accurate diagnosis of blood stream infections.

INTRODUCTION

Defined as an abnormal host immune response to infection with a pathogen in the bloodstream, sepsis occurs in 30 million people worldwide, with an estimated 6 million deaths annually[2, 3]. In the US alone, it accounts for $20B (5.2%) of annual healthcare expenditures[2]. The incidence of sepsis appears to be increasing, most likely due: (1) an aging population that becomes more susceptible as they live longer; (2) a growing number of antimicrobial-resistant (AMR) strains due to overuse of broad spectrum drugs; and (3) an increase in the number of people living with weakened immune systems caused by HIV, transplant drugs, cancer treatments, etc.

With no diagnostic tool designed specifically for sepsis, physicians generally begin treating patients with broad-spectrum drugs immediately upon onset of physical symptoms (e.g. fever, high heart/respiratory rates)[4]. In order to narrow the spectrum and provide more effective treatment, the causative pathogen must be identified and tested for antimicrobial susceptibility. Currently, this takes up to 50 hours and involves a blood draw and culture to detect growing microorganisms, classification of the Gram type to give a preliminary phenotypic ID, isolation of the microorganisms from the culture, and finally, identification (ID) and antimicrobial susceptibility testing (AST). Isolation from the blood culture necessitates a subculture requiring 18-24 hours of growth, significantly delaying ID/AST results. Sepsis is a highly dynamic illness, and thus time is critical. Early, specific treatment shows reduction in mortality rates[5]. Moreover, rapid ID/AST results avoid ineffective treatment, limit selection of resistant strains from broad-spectrum drugs, and minimize elimination of beneficial bacteria.

Becton Dickinson (BD), a worldwide leader in microbiology diagnostic solutions, holds capabilities in pathogen detection, ID, and AST. Recent work proved the feasibility of a tangential flow filtration device that isolates bacteria from the blood culture in 15 minutes, eliminating the

need for a subculture and providing a concentrated sample for rapid initiation of ID/AST. This technology evolved from a separate application however, and thus the ideal processing parameters and limitations of the system remained relatively unknown for application to rapid ID/AST.

The goal of this project involved further characterization and optimization of this technology in order to reduce processing time, maximize recovery from the blood culture, and ensure a viable input for ID/AST. We tested a variety of bacterial strains and media types in order to set a baseline for filtration performance and suitability of the output for ID/AST. This allowed us to identify weaknesses within the filtration technology and causes for poor ID/AST results. We characterized and optimized steps within the processing workflow, as well as adjusted filtration parameters based upon the results of the baseline study. This allowed us to determine the key factors of yielding quicker, more accurate ID/AST results from outputs of the technology.

BACKGROUND

While sepsis exists as one of the most common causes of death in hospitals, its diagnosis remains challenging due to the likelihood of a preexisting condition within the patient. Commonly characterized by three stages, stage one sepsis presents with a high fever and increased heart rate. As infection spreads and sepsis progresses to the second stage, symptoms include shortness of breath and organ dysfunction. The third and most severe stage is known as septic shock, and is characterized by extremely low blood pressure that leads to multiple organ failure and often death. Progression through the stages is often very quick—on the order of days or even hours—and thus time is critical. Since sepsis is most often caused by an infection of bacteria in the bloodstream, speeding up the time to a confirmatory diagnosis of the bacteria and recommendations for effective treatment is dependent upon the improvement of microbial diagnostic solutions.

Current Workflow for Diagnosis of a Blood Stream Infection

In order to develop a more effective, narrow treatment regime for sepsis patients, physicians must identify the pathogen causing the blood stream infection. The workflow for this diagnosis begins with a roughly 10mL blood draw into a culture bottle containing growth media (*Figure 1*).

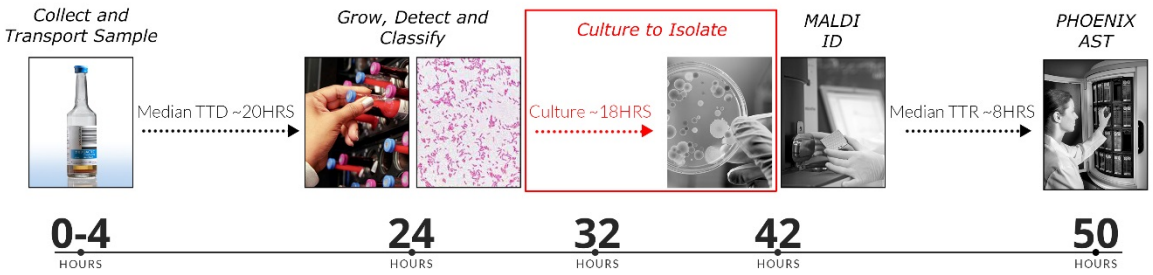

Figure 1: Current Workflow for Diagnosis of a Bloodstream Infection Based Upon use of BD Diagnostic Equipment. The current workflow for diagnosis of a bloodstream infection involves collection and transport of a blood culture (0-4 hours); incubation and detection of growth in a BACTEC instrument (20 hours); Gram staining for preliminary phenotypic identification (<1 hour); growth of a subculture to isolate pathogens (18-24 hours); MALDI ID (<1 hour); and Phoenix AST (8 hours).

Sepsis patients generally have only 10-100 CFU per 10mL blood draw, and thus the bacteria must be grown in order to confirm infection with a pathogen and yield enough material for downstream testing. For the BACTEC system, culture bottles can contain various types of growth media, such as: lytic media, which contains saponin for lysing blood cells and releasing intracellular pathogens; PLUS media, which contains ion-exchange resin beads that sequester any antibiotics already present in the patient that inhibit bacterial growth; and standard aerobic media, which provides growth for aerobes. After collection and transport of the samples to an automated blood culture instrument (e.g. BACTEC), the instrument incubates and continuously monitors the samples in order to detect growth. The median time to detection (TTD) for bacteria is 20 hours.

Once growth is detected (generally at about 10^8 CFU/mL), the culture, now known as a positive blood culture (PBC), is removed and a Gram stain is performed. This involves chemical

staining of an aliquot of the PBC and gives a preliminary identification of the bacteria based on phenotype. Additionally, it allows for identification of a polymicrobial infection. The Gram stain classifies bacteria as Gram negative or Gram positive. Gram positive bacteria tend to clump together and appear larger than Gram negative bacteria, which appear as rods. Following the Gram stain, the bacteria must be isolated from the PBC by plating an aliquot onto a growth plate (i.e. purity plate). This isolation step is key to produce a viable input for ID/AST methods; however, the length required for growth necessitates the development of more rapid isolation methods. From the isolate, a matrix-assisted laser desorption/ionization time-of-flight mass spectrometry (MALDI ToF MS, or MALDI) ID can be made within a few minutes, followed by AST. Although the detailed mechanisms of MALDI ID and AST are beyond the scope of this work, it is important to understand the basic underlying principles and analyses of results in order to understand how to optimize the output of PBC processing for downstream testing.

Antimicrobial Susceptibility Testing

Antimicrobial susceptibility testing (AST) is critical in order to provide accurate, specific recommendations for prescribing effective treatment. It allows physicians to narrow treatment from broad spectrum antimicrobials to specific concentrations of drugs necessary to kill the infective bacteria. Common AST platforms utilize a broth dilution technique, which exposes the bacteria to decreasing concentrations of antimicrobial agents in liquid media. Phoenix panels are plastic microdilution trays that contain several rows of various dried antimicrobial agents. Each row contains 5 twofold serial dilutions (doubling dilutions) of the same antimicrobial agent. Upon inoculation of the panel with a redox indicator-bacteria solution and incubation within the instrument, Phoenix continuously measures changes in both the redox indicator and turbidity of the solution in order to detect growth of the bacteria.

The minimal inhibitory concentration (MIC), defined by the lowest doubling dilution in which no visible growth occurs, quantifies growth of bacteria in an AST panel. Interpretation of AST results include two forms. The first defines isolate MICs as being in **essential agreement** with the regulatory-defined reference MIC of the specific pathogen. Isolates that produce an essential agreement fall within ±1 doubling dilution of the reference. The second form calls bacteria susceptible (S), intermediate (I), or resistant (R) to the antimicrobial based upon its MIC. The bacteria get further defined as being in **categorical agreement** if it yields the same category (S, I, or R). For the scope of this project, we focused only on interpretation of results using essential agreements. For part of the validation of medical devices for AST, the FDA requires ≥90% of test samples to be in essential agreement[6].

Identification of Pathogens using MALDI-ToF MS

Identification of pathogens is key to accurately interpreting AST results and providing precise treatment. MALDI is rapidly expanding as a fast, labor-inexpensive method for microbial identification. MALDI entails ionization of the test isolate peptides by short laser pulses, which create charged molecules that travel up a flight tube within the instrument[7, 8]. The instrument measures the time of flight and creates a peptide mass fingerprint (PMP) that is compared to a database for an ID. Analytes are given an identification based upon the yielded spectra and the match score. Based upon Bruker Daltonic's recommendations, a score from 0 to 1.69 yields no reliable identification, a score from 1.70 to 1.99 yields a genus-level match, and a score of 2.00 or greater yields a species-level match[9].

Sample preparation for MALDI is relatively simple, but crucial in order to generate accurate results. After applying the sample to the target plate, pre-treatment with a strong organic acid (e.g. ethanol, formic acid) is critical in order to extract intracellular proteins and remove

contaminants. Contaminants may interfere with even sample crystallization within the matrix, resulting in low resolution and low identification accuracy. Furthermore, an excess of salts in the sample may create a spectrum that dwarfs the desired spectra. Alternatively, protein extraction from the sample can be performed prior to application to the plate. This generally provides a cleaner sample and allows for more thorough extraction, but is more time consuming as it requires various centrifugation and elution steps. Pretreatment and extraction precede application of the matrix, which includes energy-absorbent organic compounds[7, 10]. Once dry, the matrix co-crystallizes the sample and serves to adsorb and transfer energy from the laser pulses to the sample.

Positive Blood Culture Processing Approach: Separation via Tangential Flow Filtration

The main components of a positive blood culture include red and white blood cells in addition to bacteria. As seen in *Figure 2*, both red and white blood cells are more than triple the size of a Gram negative bacterial rod.

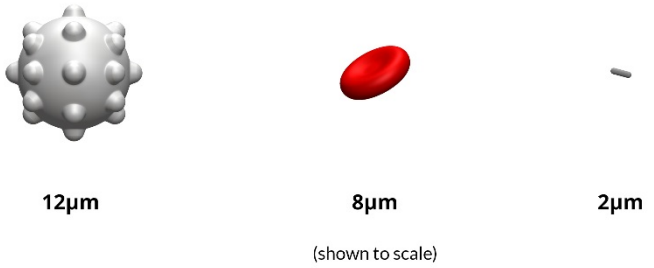

Figure 2: Main Components of a PBC. Shown to scale from left to right: white blood cell, red blood cell, and Gram negative rod.

Using a polycarbonate track-etched membranes (TEM) with a pore diameter close to that of bacteria, tangential flow filtration (TFF) can be applied in order to exclude the blood background and collect only the desired pathogen (*Figure 3*).

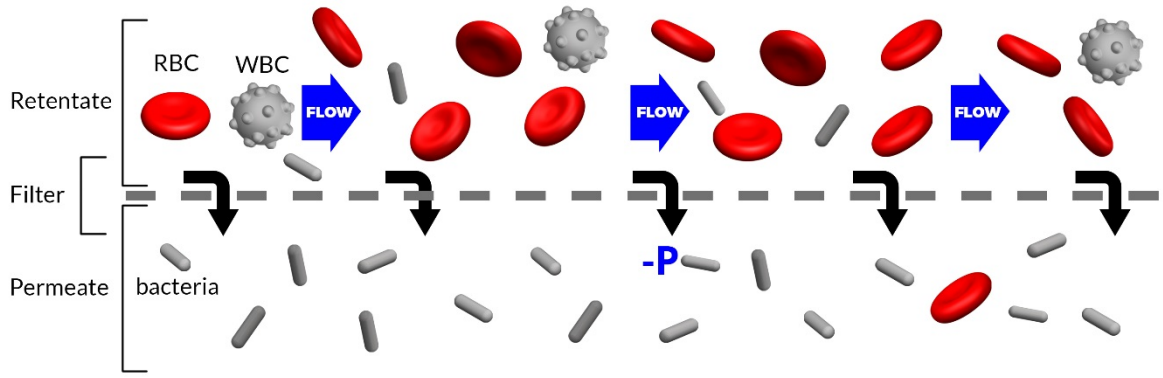

Figure 3: Tangential Flow Filtration of a Positive Blood Culture. A positive blood culture flows across a track-etched membrane via a peristaltic pump. A vacuum pump creates a pressure gradient that draws the desired pathogen through the TEM pores while excluding the blood background.

In the PBC processing technology, the sample flows tangentially across the TEM via a peristaltic pump, preventing pore clogging. Meanwhile, a vacuum pump creates a pressure gradient to draw the bacteria into a collection tube. The retentate, i.e. blood background and any remaining bacteria, gets recycled through the apparatus until the entire sample runs through the filter.

Previous Work with TEM-TFF Technology

Previously, BD applied this technology to rapid separation of plasma from whole blood. With the need to eliminate an 18-hour subculture step in the diagnostic workflow, they then applied TFF to separation of bacteria from whole blood. Studies confirmed the feasibility of this application by processing nine types of microorganisms grown in standard aerobic media. Results showed a significantly reduced workflow timeline of 32 hours from culture inoculation (i.e. blood draw) to accurate ID/AST results, allowing movement into the technical development phase. This being said, parameters for PBC processing were selected based upon the original intent (plasma separation) of the TFF technology with a limited battery of organisms and media types. This chapter details results from an expanded test list of organisms across more than one media type, as well as methods and results of processing characterization and optimization. Overall, the scope

of this project aimed to understand the impact of various factors of the blood culture input and sample processing workflow on ID/AST.

EXPERIMENTAL METHODS

Understanding the impact of processing parameters on downstream testing results is key to optimizing bacterial recovery for accurate ID/AST. We conducted a study on an expanded repertoire of organisms and media types to set a baseline of technology performance for downstream testing. From this study, we targeted problematic areas within the workflow. This allowed us to characterize and optimize various parameters in order to increase processing efficiency and yield a more suitable output for ID/AST.

PBC Processing Workflow

Figure 4 shows the general workflow for processing a PBC.

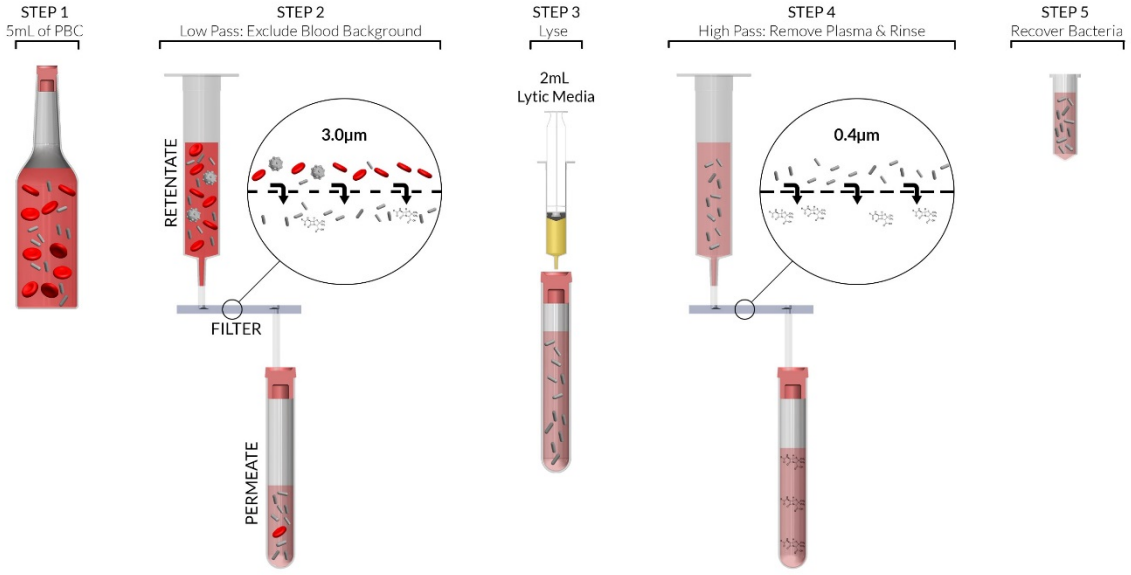

Figure 4: General Workflow for Separation of Bacteria from a Positive Blood Culture (Positive Blood Culture Processing). Step 1: 5mL aliquot drawn from PBC. **Step 2:** Sample run through 3.0µm filter and washed with 5mL DI water to exclude blood background. **Step 3:** 2mL of BD BACTEC Lytic Anaerobic media added to permeate. **Step 4:** Sample run through 0.4µm filter to exclude plasma and cellular debris, and washed with 5mL DI water. **Step 5:** Bacteria suspended in DI water with approximately 1mL of wash remaining, and retentate collected in 2mL Eppendorf tube.

After inverting the PBC several times to ensure a well-mixed culture, a 5mL aliquot was drawn from the PBC bottle using a 5mL syringe and 18G needle. The flowrate of the peristaltic pump and pressure of the vacuum pump were set to 25mL/min and -70kPa, respectively, and the apparatus was turned on. The PBC aliquot was dispensed into the apparatus and run through a 3µm filter in order to exclude the blood background. A 5mL deionized (DI) water wash was applied to the sample as it ran through in order to prevent buildup on the membrane and aid flow of bacteria through the pores. We collected the permeate of this step once the entire blood background was visibly excluded, or with about 1mL of retentate remaining. 2mL of lytic anaerobic media were then added to the permeate in order to lyse any blood cells that passed through the filter. This sample was run through a 0.4µm filter using the same pressure and flowrate in order to further isolate the bacteria from plasma and remaining cellular debris. Another 5mL deionized (DI) water wash was applied to aid filtration. After completing the wash, the sample was collected in a 2mL Eppendorf tube and analyzed the output using downstream tests.

Baseline Data

We collected downstream testing data in order to set a baseline for initial performance across a larger battery of microorganisms and media than previous studies. We processed thirty strains of bacteria (see Appendix *1, Table A1*) grown in each of the following BACTEC media: Standard Aerobic, Lytic Anaerobic, and PLUS Aerobic.

Initial performance assessments included analysis of the percent recovery of bacteria from the original PBC, Phoenix AST results compared to the reference method (purity plate), and capability and accuracy of ID using MALDI-ToF MS. *Figure 5* illustrates the experimental setup for collection of baseline data, defined in detail by the following methods:

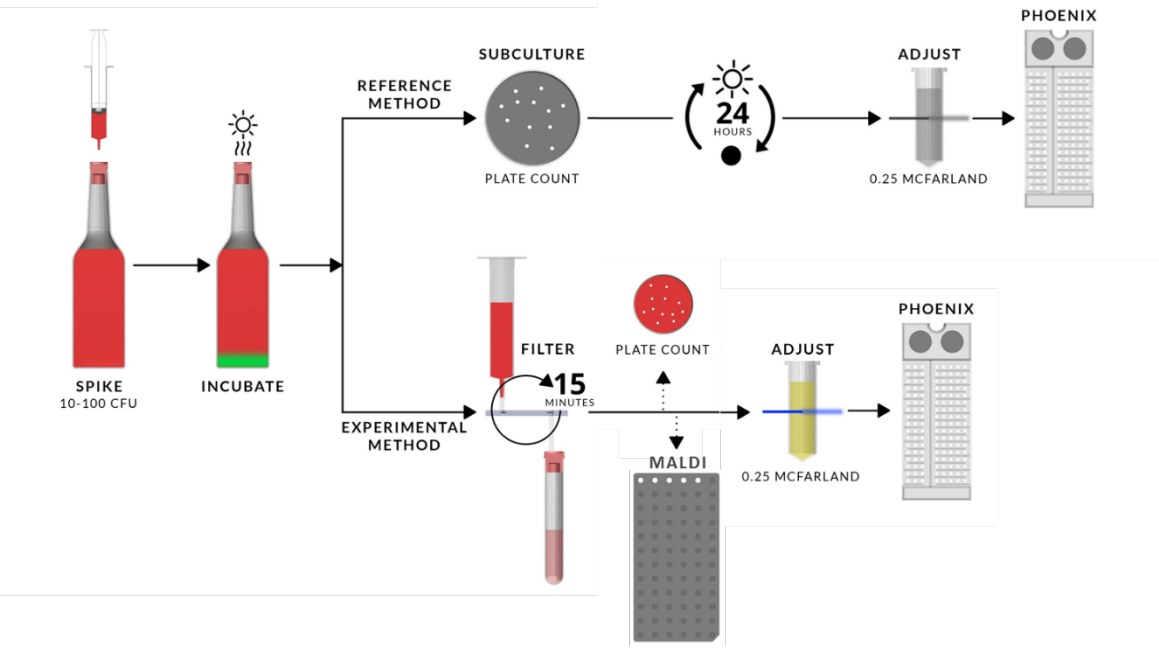

Figure 5: Workflow of Baseline Testing and General Protocol for Downstream Testing. We spiked BACTEC Blood Culture Media bottles with 40mL and 10-100 CFU for each microorganism and media type. Blood cultures incubated overnight in BACTEC FX instruments. After the instrument detected bacterial growth, we removed the blood cultures and processed them through both the reference and experimental methods. For the reference method, we removed an aliquot of PBC for a subculture, which we incubated for 24 hours before performing plate counts and Phoenix AST. For the experimental method, we processed the PBC through the standard processing workflow, plated the output tube for plate counts, and ran MALDI and Phoenix AST directly from the output tube. For deviations from the standard PBC processing method, see subsequent experimental methods.

Simulation of Positive Blood Culture. We simulated a positive blood culture from a sepsis patient by inoculating BACTEC blood culture bottles with 10 mL of blood and 10-100 CFU. In order to do so, for each strain of bacteria, we made a subculture from a QC plate 24 hours prior to inoculation. From this subculture, we created a 1 McFarland solution with sterile saline and made 100-fold serial dilutions using standard aerobic media to reach a dilution factor of 10^{-6}. We then inoculated a new BACTEC blood culture bottle of the specified media type with 10mL of blood (warmed to room temperature) followed by 0.1mL of the 10^{-6} dilution sample. We incubated the blood cultures overnight in a BD BACTEC FX instrument.

Positive Blood Culture Processing. We followed the standard sample processing workflow shown in *Figure 4*.

Cell Plating and Plate Counts. Prior to processing, we plated an aliquot of the PBC for the reference method. We also plated the output tube from processing. For plating and counting of all samples, we used the dilution scheme and calculations shown in *Appendix 1, Table A1.2*.

AST Processing using Phoenix. We processed both the experimental and reference method samples for AST according to the BD Phoenix System User's Manual protocol[11]. Briefly, we used Phoenix ID broth to make a 0.5-0.6 McFarland for each sample. We then added 42µL of AST indicator and 25µL of the 0.5-0.6 McFarland to a Phoenix AST broth tube (8mL) and inoculated an AST-only panel specific to the type of bacteria. For the experimental method, if the standard 0.5-0.6 McFarland could not be achieved for AST panel inoculation, we adjusted the sample to a 0.25-0.3 McFarland using Phoenix ID broth and added 50µL to the AST broth.

Identification using MALDI-ToF MS. We used a MALDI Biotyper (Bruker Daltonics) to identify all samples throughout the entirety of this project. For each plate processed, we included two spots of Bacterial Test Standard (BTS) for a performance control. BTS contains an extract of *E. coli* DH5 alpha and two other high molecular weight proteins, mixed with a standard solvent (50% acetonitrile, 47.5% water, 2.5% trifluoroacetic acid)[12, 13]. This mixture yields a peptide and protein profile that covers the entire range of spectra identified by the instrument, thus serving as a quality control standard. For samples processed through the experimental method, we pipetted two 1µL layers directly from the output tube onto a spot on the stainless steel MALDI target plate. On top of each test spot, we pipetted 1µL of formic acid and incubated the plate at 35°C until the spots dried. Finally, we pipetted 1µL of matrix on each test spot, allowed them to dry at room temperature, and ran the plate on the instrument.

Filtration of Resin Beads from PLUS Aerobic PBCs

BACTEC PLUS Aerobic blood culture bottles contain resin beads large enough to clog the pores of the TEM filters, effectively inhibiting filtration of bacteria. In order to prevent this, we used a 100µm mesh filter to remove as many resin beads as possible from the PBC before drawing an aliquot for filtration. To confirm no bacterial loss during this filtration, we spiked four PLUS Aerobic culture bottles, two with wild type *E. coli* and two with wild type *S. aureus*, according to the baseline study workflow method and incubated overnight. Once the cultures turned positive, we used a 100µm mesh filter held in place with a syringe filter holder to filter the PBC into a vacutainer. For each bacterium, we collected three BD vacutainers of sample, processed each vacutainer through the PBC processing workflow, and plated the outputs according to the dilution scheme described in the baseline study methods.

Optimization of Lysis Step

Previously, the material and amount of lytic agent used was selected based upon the amount of saponin present in BACTEC Lytic Anaerobic media (2mL of 2.6g/L saponin). In order to determine the optimal amount of saponin and eliminate the addition of unnecessary media components into the processed sample, we compared the ability of varying concentrations of saponin water to yield accurate downstream results. We processed five PBCs spiked with wildtype *E. coli*. For each sample, we applied a different concentration of lytic agent. We used 2mL of lytic anaerobic media as a positive control, 2mL 1.3g/L saponin, 2mL 2.6g/L saponin, 2mL 3.9g/L saponin, and 2mL 5.2g/L saponin. We used identification scores from MALDI to analyze the results and characterize the effects.

Characterization of Flux across Filter over Time

Studies show that over time, a cake layer of filtrate forms on the top of filter membranes used in dead-end filtration, blocking material from flowing through the pores[13, 14]. Although this buildup is shown to decrease by switching to TFF, we hypothesized that any cake layer formation on the filter causes a decrease in the flux across the filter over time, thus limiting the collection and concentration of bacteria from the original sample. To characterize the flux across our filter membranes, we used a scale to measure the weight of the retentate over time. We used Matlab to collect the scale readings and convert them to volume before generating a plot of flux over time. We collected data for flux across both the 3µm and 0.4 µm filters for *S. epidermidis* (ATCC 14990), *E. faecalis* (ATCC 51299), *S. aureus* (CDC Challenge 2052), and *S. lugdunesis* (clinical).

Effects of Increased Pore Size on Downstream Testing Results

We hypothesized that increasing the pore size of the first filtration step increases the flux of the sample across the membrane, thus increasing recovery of bacteria and improving downstream testing results. We quantified the passage of red blood cells through various filter pore sizes in order to determine the tolerance of downstream tests to red blood cells and blood background.

Bacterial Recovery. While processing the PLUS Aerobic blood cultures during the baseline study, we processed all samples through a 5µm first stage filtration and a 0.8µm second stage, in addition to the 3µm/0.4µm filtration scheme used for all media types. We followed the same baseline study and PBC processing workflows and collected the same data.

Passage of Red Blood Cells. We used a hemocytometer to quantify red blood cell passage through filters of varying pore sizes. We incubated 10mL of blood in 40mL Standard Aerobic media overnight in a BACTEC to simulate a negative blood culture (NBC). We then processed three 5mL

aliquots of the NBC through a 5μm filter. We made three 10-fold serial dilutions from each permeate, as well as from a 5mL aliquot of the NBC (unfiltered). We pipetted 10μL of each 10^{-3} dilution onto a bright line hemocytometer (AO Scientific Instruments) and counted the number of red blood cells using an inverted microscope.

RESULTS

Due to the large number of samples processed during the baseline study, we encountered a number of difficulties with the processing of certain media types and bacteria. We characterized and adjusted steps of the PBC processing workflow in order to yield accurate results for the baseline study. From this study we found that overall, Gram negative bacteria perform well across all media types in terms of filtration, AST, and MALDI ID performance. Gram positive bacteria, specifically *Staphylococci*, proved problematic in yielding accurate ID/AST results across all media types. We attributed this to a lack of bacteria in the output due to a combination of cake layer formation on the membrane surface, which impedes filtration, and the clumping nature of Gram positive bacteria. After characterizing the flux across filter membranes, we found that over time flux remains relatively constant for larger pores, while smaller pores show a decrease in flux. This suggests a smaller cake buildup and higher filtration rate as pore size is increased. Furthermore, we found that increasing the pore size allows recovery of more Gram positive bacteria and improves ID/AST results.

PBC Processing Workflow

During the initial phases of the baseline study, we encountered inaccurate downstream results. Thus, we targeted certain processing steps in order to improve the quality of the output tube for more accurate ID/AST results.

Wash Steps. While processing the first round of PBCs (Standard Aerobic media), we observed a dark pink to red color in the permeate from the first filtration step. Since this initial step serves to separate the blood background out from the sample, it should appear relatively clear with little to no red coloring. We hypothesized that the discoloration resulted from premature lysis of red blood cells due to an increase in osmotic pressure caused by immediate washing of the sample with 5mL DI water. We began washing samples with 5mL of sterile saline rather than DI water. Furthermore, we processed samples through the workflow, diluting the PBC aliquot upfront with 5mL of saline before filtering the sample rather than applying a wash during the first filtration step. This cleaned up the samples significantly and the permeate appeared relatively colorless.

Optimization of Lysis Step. We targeted the lysis step of PBC processing in order to further eliminate as much blood background as possible from the final output sample. Since residual blood background in the output is most likely to interfere with proper ID of bacteria, we compared MALDI ID scores for each lytic agent in order to determine the optimal concentration of saponin (*Figure 6*). We used Lytic Anaerobic Media as a positive control. The highest average scores came from the Lytic Anaerobic media (2.36) and 2.6g/L saponin (2.31), which is the concentration of saponin present in the lytic media. The 1.3g/L saponin yielded an average score of <1.70, i.e. not a reliable ID. While the 3.9g/L saponin yielded a score with species-level accuracy, it was over 0.3 points lower than the lytic media. The 5.2g/L saponin yielded about the same score as 2.6g/L (2.2765 versus 2.31, respectively).

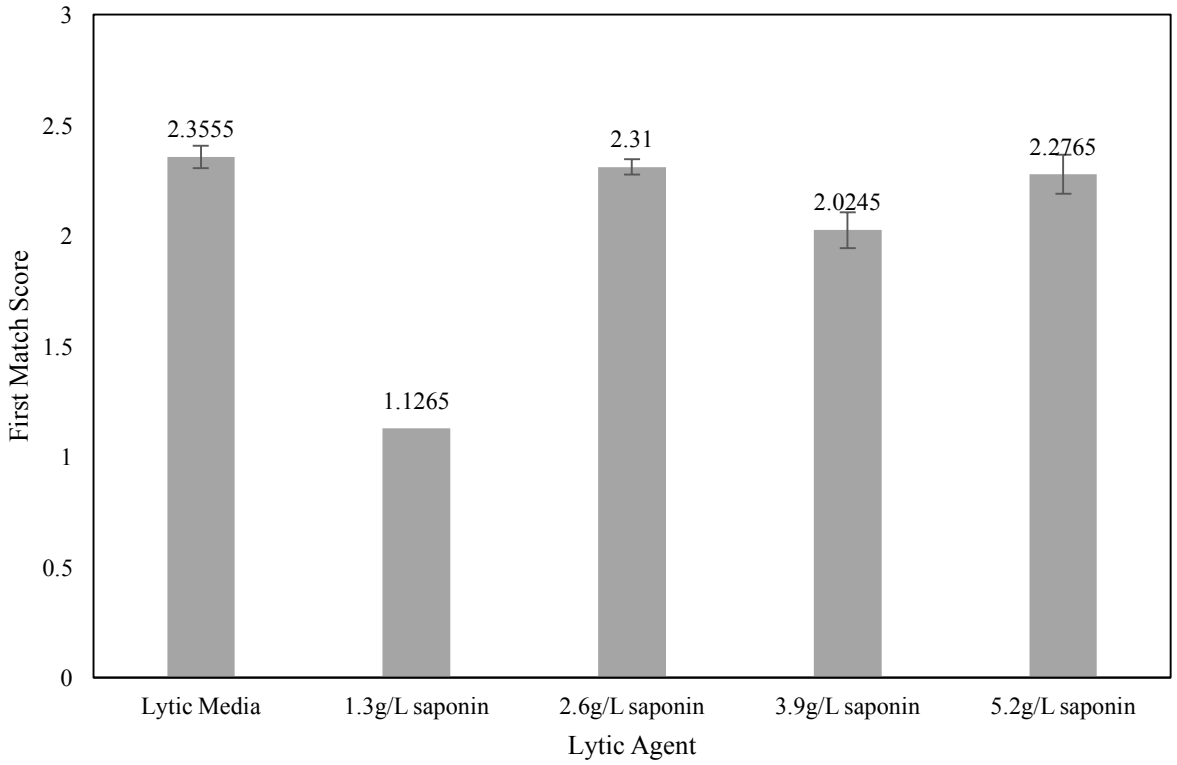

Figure 6: First Match MALDI ID Scores for Processed E. coli PBCs using Varying Lytic Agents. We processed a PBC containing *E. coli* (ATCC 25922) using Lytic Anaerobic media (postiive control) and varying concentrations of saponin as lytic agents. We processed duplicates for each lytic agent and averaged the first match scores, shown above.

This indicates that the lowest concentration of saponin is insufficient in removing enough background from the sample and thus the final output likely contains material that interferes with ID of bacteria. Furthermore, while saponin concentrations of 3.9 and 5.2g/L yield sufficient results, we moved forward with the 2.6g/L saponin in order to minimize the amount of material used.

In order to further confirm that 2.6g/L saponin water performs the same or better than the original lytic agent, we processed samples from the baseline study using both BACTEC Lytic Anaerobic media and 2.6g/L saponin water. We compared the MALDI scores of each lytic agent by performing a two-sample t-test, which yielded average ID scores of 2.2398 and 2.2068 for 2.6g/L saponin and lytic media, respectively; a difference of 0.033; and a p-value of 0.401 (*Figure 7*).

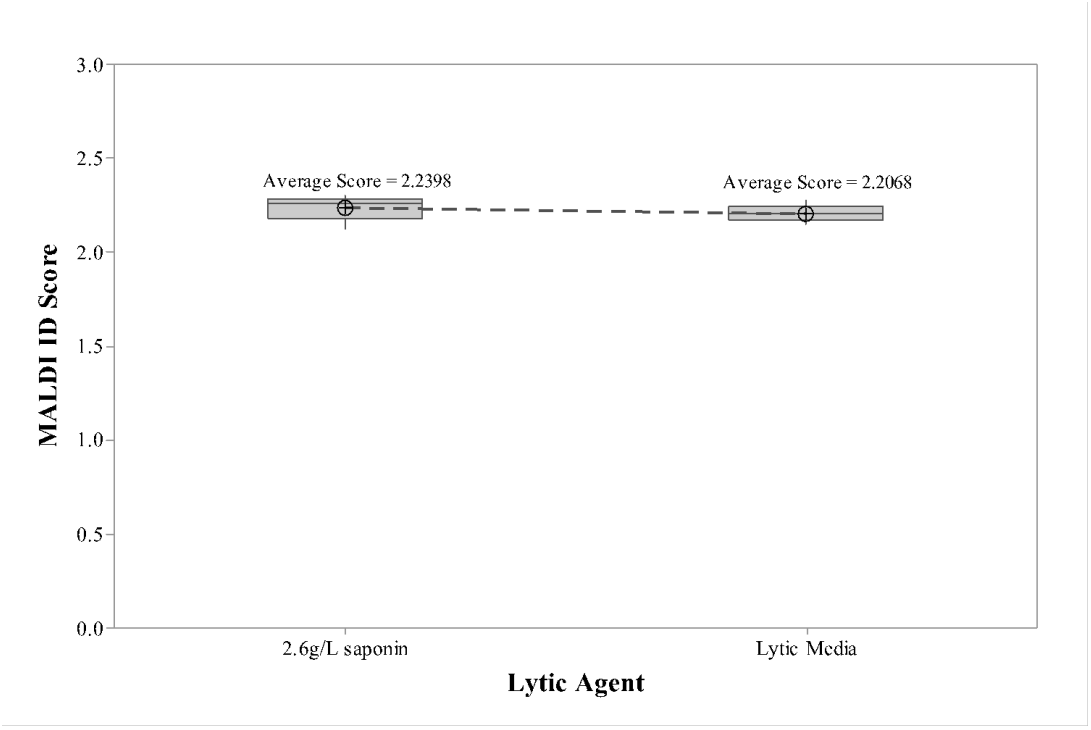

Figure 7: Distribution of First Match MALDI Scores of Baseline Test Isolates using Lytic Anaerobic Media vs. 2.6g/L Saponin as a Lytic Agent. We processed 2 aliquots each from 5 PBCs from the baseline test microorganisms (*E. coli*, *P. aeruginosa*, *E. faecalis*, *S. aureus*, and *S. pneumoniae*) using Lytic Anerobic Media and 2.6g/L saponin for lytic agents. We performed a two-sample t-test in order to observe any significant difference in the MALDI ID scores from using media versus saponin. We found no significant difference as $p>0.05$.

With these results, we confirmed that at a significance level of 0.05, there is no significant difference between using 2.6g/L saponin versus lytic media. Furthermore, both lytic agents yielded average scores sufficient for a species level match (≥2.0), signifying their abilities to lyse enough blood background for accurate ID. Thus, we moved forward with using 2.6g/L saponin in place of lytic media during PBC processing.

Processing of Lytic Anaerobic PBCs. We also observed pink-red discoloration in the output tubes of the Lytic Anaerobic PBCs and subsequent incapability of accurate MALDI ID for these samples. We hypothesized that this discoloration stemmed from lysis of blood cells by the saponin present in the lytic media. We ran five samples through the full PBC processing workflow, applying as much DI water as necessary to yield a cleaner output sample. We did not observe any significant

increase in output sample clarity until we used at least 10mL of DI water during the second wash step. In order to maintain short processing time, we did not implement an increased wash volume. Instead, we allowed the sample to run almost entirely through the second filtration step before slowly applying the 5mL wash. This improved sample clarity from application of the DI water wash at the beginning of the second filtration step.

Removal of Resin Beads from PLUS Aerobic PBCs. We drew three aliquots from each PBC through a syringe filter, and averaged the plate counts over each microorganism. The *E. coli* samples averaged a 10% increase after resin bead removal while the *S. aureus* samples averaged a 25% loss in bacteria (*Figure 8*).

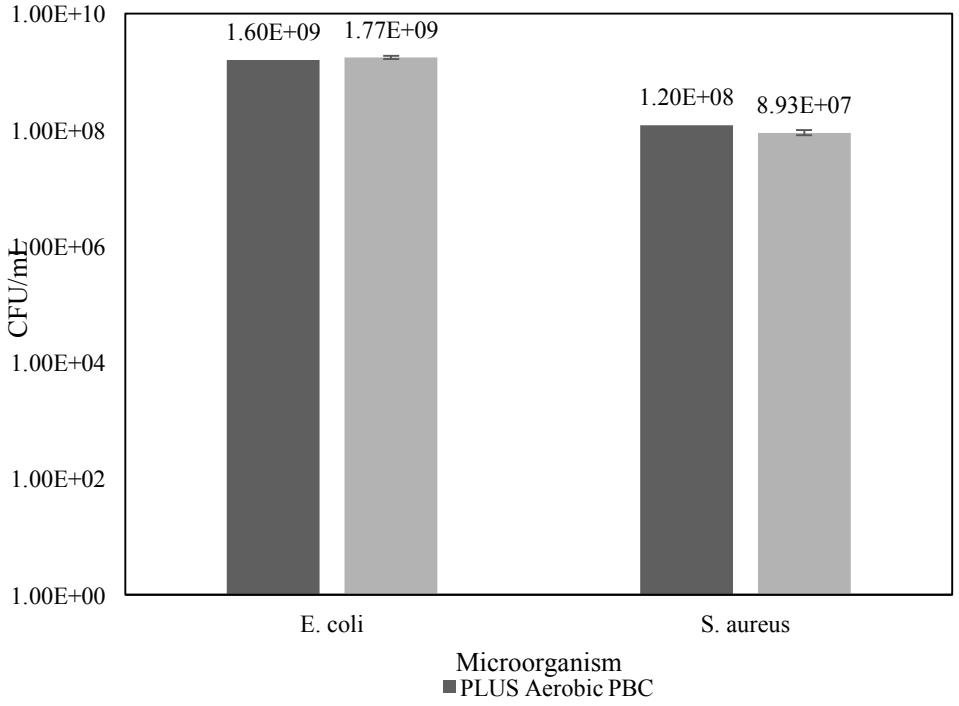

Figure 8: Loss of Bacteria from Filtration of Resin Beads from PLUS Aerobic PBC. We used a syringe filter to remove the resin beads from PLUS Aerobic PBCs in order to prevent membrane fouling during PBC processing. We plated two separate PBCs containing *E. coli* (ATCC 25922) and *S. aureus* (ATCC 29213) after the BACTEC instrument detected them as positive. We then filtered out the resin beads and plated this PBC to observe any bacterial loss.

Even with a 25% loss of bacteria from the *S. aureus* sample, the difference remains less than half of a log from the original PBC. Moreover, we recorded values on the order of $8x10^7$ CFU/mL for *S. aureus* grown in Standard Aerobic and Lytic Anaerobic media during the baseline study. In order to verify that filtering resin beads prior to processing does not significantly affect the number of viable bacteria, we performed a two-sample t-test and yielded a p-value of 0.895. For a significance level of 0.05, this confirmed that removing resin beads from PLUS Aerobic samples leaves the PBC unaltered from its original state while making it more suitable for processing. We implemented this procedure for all PLUS Aerobic samples processed during the baseline study.

Baseline Performance Data

We collected and analyzed data to evaluate filtration performance, capability and accuracy of ID by MALDI, and accuracy of Phoenix AST compared to the reference method.

Filtration Performance. For each bacteria and media type, we averaged the plate counts of the original PBC and output tube across strains (*Appendix 1, Figure A1.1*). We compared these values by calculating the percent recovery for each microorganism in each media type. Overall, we recovered an average of 80.0%, 93.4%, and 98.5% of bacteria from Gram negative and 48.3%, 79.5%, and 76.8% of bacteria from Gram Positive PBCs grown in Standard Aerobic, Lytic Anaerobic, and PLUS Aerobic media, respectively (*Figure 9*). Gram negative microorganisms *A. baumanii* and *P. aeruginosa* did not grow in Lytic Anaerobic media due to their aerobic nature, and thus we did not yield any downstream test results for these microorganisms.

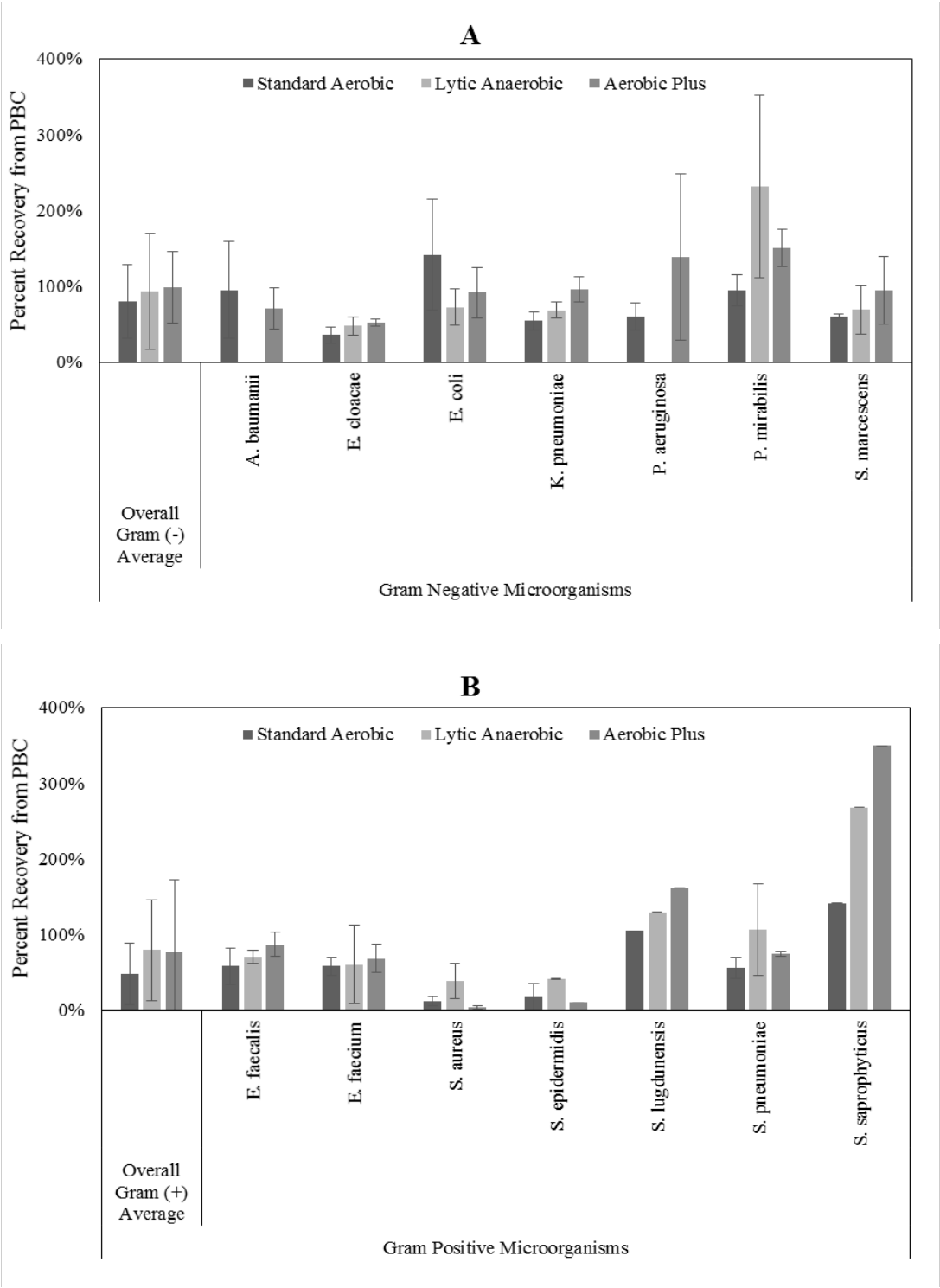

Figure 9: Total CFU in PBC vs. Output Tube for Gram Negative Bacteria for Each Media Type. We averaged the PBC and output plate counts across the strains of each microorganism for each type of media, and then used these counts to calculate the percent recovery of bacteria from filtration. (A) Standard Aerobic Media. (B) Lytic Anaerobic Media. **(Note: BACTEC detected no growth for *A. baumanii* and *P. aeruginosa* in Lytic Anaerobic media due to their aerobic nature)**. (C) PLUS Aerobic Media. (D) Percent recovery per media type for each Gram negative bacteria.

In general, the Gram positive bacteria—specifically *Staphylococci*—yielded a much lower percent recovery than the Gram negative bacteria. Additionally, bacteria grown in Lytic Anaerobic and PLUS Aerobic yielded higher percent recoveries (overall averages of 85.9% and 88.8%, respectively) than Standard Aerobic media (overall average of 65.2%). This being said, for most bacteria with a lower than average percent recovery, the difference in total CFU from PBC to output remained within one log and greater than 10^8 CFU. *Staphylococci* persisted as an exception. In order to qualify low percent recoveries and better understand an acceptable lower limit, we looked further to the results of ID and AST.

Phoenix AST Performance. We compared Phoenix AST results of the output samples to results of an isolate from the original PBC. We used the MICs from the original PBC isolate as a reference and calculated the difference in doubling dilutions of the output sample from the reference. Across all media types and microorganisms 97.3% of all samples gave an essential agreement. *Table 1* displays essential agreement data for each microorganism in each media type.

Table 1: Phoenix AST Results for Each Microorganism and Media Type.

Microorganism	# of Strains	Standard Aerobic		Lytic Anaerobic		PLUS Aerobic	
		Total n	Essential	Total n	Essential	Total n	Essential
Gram Negative	**16**	**463**	**95.90%**	**347**	**98.85%**	**463**	**99.14%**
A. baumanii	2	58	98.28%	No BACTEC growth	N/A	58	96.55%
E. cloacae	2	58	98.28%	58	96.55%	58	100.00%
E. coli	3	87	82.76%	87	100.00%	87	100.00%
K. pneumoniae	3	87	100.00%	87	98.85%	87	98.85%
P. mirabilis	2	58	100.00%	58	100.00%	58	100.00%
P. aeruginosa	2	58	96.55%	No BACTEC growth	N/A	58	100.00%
S. marcescens	2	57	100.00%	57	98.25%	57	98.25%
Gram Positive	**14**	**374**	**89.84%**	**436**	**83.03%**	**605**	**89.09%**
E. faecalis	2	68	95.59%	68	95.59%	68	95.59%
E. faecium	2	34	100.00%	68	100.00%	102	94.12%
S. aureus	4	136	99.26%	136	97.79%	204	98.04%
S. epidermidis	2	68	50.00%	68	0.00%	101	49.50%
S. lugdunensis	1	34	100.00%	34	100.00%	34	100.00%

S. saprophyticus	1	34	100.00%	34	100.00%	68	100.00%
S. pneumoniae	2	*not tested	*not tested	28	100.00%	28	92.86%
Overall Total	**30**	**837**	**93.19%**	**783**	**90.04%**	**1068**	**93.45%**

Gram negative bacteria yielded concordant results with the reference method across all media types. For gram positive bacteria, *S. epidermidis* posed the biggest challenge. For all three media types, the output of the wildtype strain PBC did not grow in the AST panel. Additionally, the wildtype isolates from PLUS Aerobic media that we used as a reference did not grow in the panel. We reran both the reference and the output through AST, but again yielded no growth. No growth from reference samples most likely signifies a contaminated or old QC plate since the sample was unprocessed. For *S. epidermidis* PBCs grown in lytic media, neither the outputs from the wildtype nor resistant strains grew in AST. The remaining *Staphylococci* did not pose as much of a challenge for AST, as they all yielded at least 97.79% concordance with the reference method.

MALDI ID Performance. We collected identification data for 91 outputs from PBC processing across three media types (*Table 2*). We grouped isolate scores into three levels of accuracy based upon recommendations from Bruker. Of the 46 Gram negative isolates tested, 93.5% (n=43) identified correctly to the genus level, 91.3% (n=42) to the species level, and 6.5% (n=3) yielded no reliable identification. For the 45 Gram positive isolates,71.1% (n=32) identified correctly to the genus level, 53.3% (n=24) to the species level, and 28.9% (n=13) yielded an unreliable identification.

Table 2: Performance of MALDI Biotyper for ID of Each Microorganism (Total across Strains and Media Types).

Microorganism	Total Number of Isolates	Accuracy of ID, n (%)		
		Species Correct	Genus Correct	No ID
Gram Negative	**46**	**42 (91.3%)**	**43 (93.5%)**	**3 (6.5%)**
Acinetobacter baumannii	4	4 (100%)	4 (100%)	0 (0%)
Enterobacter cloacae	6	5 (83.3%)	6 (100%)	0 (0%)
Escherichia coli	10	9 (90.0%)	9 (90.0%)	1 (10.0%)
Klebsiella pneumoniae	9	8 (88.9%)	8 (88.9%)	1 (11.1%)

Proteus mirabilis	6	6 (100%)	6 (100%)	0 (0%)
Serratia marcescens	7	6 (85.7%)	6 (85.7%)	1 (14.3%)
Pseudomonas aeruginosa	4	4 (100%)	4 (100%)	0 (0%)
Gram Positive	**45**	**24 (53.3%)**	**32 (71.1%)**	**13 (28.9%)**
Staphylococcus aureus	13	5 (38.5%)	9 (69.2%)	4 (30.7%)
Staphylococcus epidermidis	5	0 (0.0%)	1 (20.0%)	4 (80.0%)
Staphylococcus lugdunensis	3	0 (0%)	1 (33.3%)	2 (66.7%)
Staphylococcus saprophyticus	5	2 (40.0%)	3 (60.0%)	2 (40.0%)
Enterococcus faecium	7	6 (85.7%)	6 (85.7%)	1 (14.3%)
Enterococcus faecalis	6	6 (100%)	6 (100%)	0 (0%)
Streptococcus pneumoniae	6	5 (83.3%)	6 (100%)	0 (0%)
Grand Total	**91**	**66 (72.5%)**	**75 (82.4%)**	**16 (17.6%)**

For isolates that yielded "No Peaks Found" (i.e. a score between 0 and 1.70, exclusive) upon the initial run, we added layers of sample as necessary in order to determine if the cause stemmed from lack of bacteria. We added up to three additional 1μL layers. Overall, MALDI identified Gram negative microorganisms more accurately than Gram positive microorganisms. *Staphylococci* strains in particular yielded poor ID accuracy, with 46.2% (n=12) yielding no reliable identification.

Looking further at MALDI accuracy across media types, we saw accurate identification for all Gram negative samples in both Standard and PLUS Aerobic media; however, 21% (n=3) of the strains grown in Lytic Anaerobic media yielded no reliable identification (*Figure10 A*). For Gram positive bacteria, 54% (n=7) grown in Standard Aerobic, 78% (n=11) grown in Lytic Anaerobic, and 77% (n=14) grown in PLUS Aerobic media identified correctly to the genus level (*Figure 10 B*).

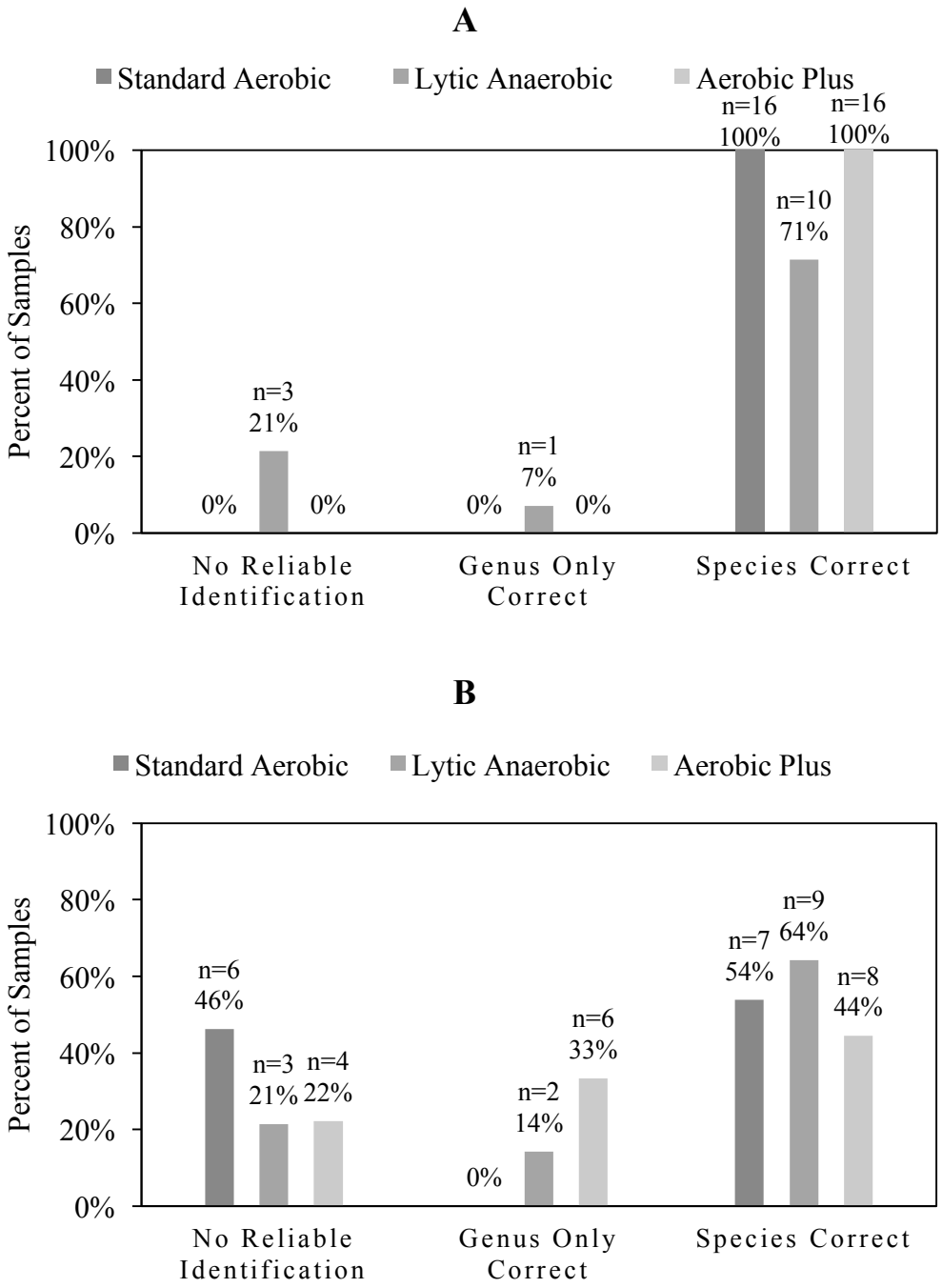

Figure 10: Distribution of MALDI ID Accuracy per Media Type. (A) Accuracy of ID per media type for Gram negative microorganisms **(B)** Accuracy of ID per media type for Gram positive microorganisms.

In general, we experienced difficulty accurately identifying the PBC processing outputs of Gram positive bacteria (namely *Staphylococci*) and outputs from Lytic Anaerobic PBCs.

Characterization of Flux Across the Membrane over Time

We hypothesized that the difficulties with MALDI ID and Phoenix AST stems largely from a lack of viable bacteria in the output due to poor flow across and through the membrane. Thus, we characterized the flux across the filter membrane in order to understand any changes in the level of filtration over time. We filtered PBCs through membranes with 3µm pores and membranes with 0.4µm pores. We calculated the flux across the filter membrane from the volume of permeate collected on a scale. We plotted the flux over time for each sample and pore size (*Figure 11*).

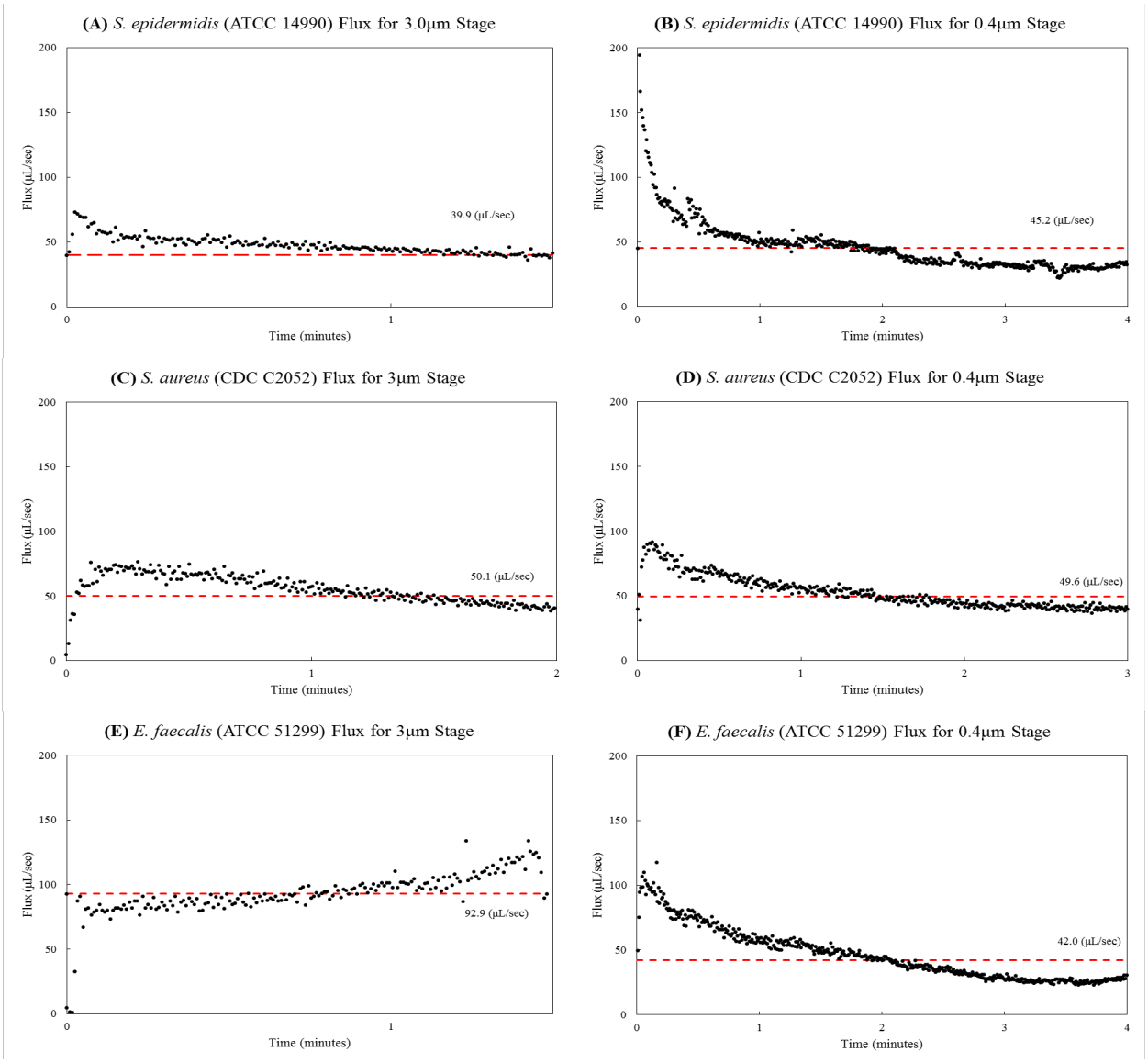

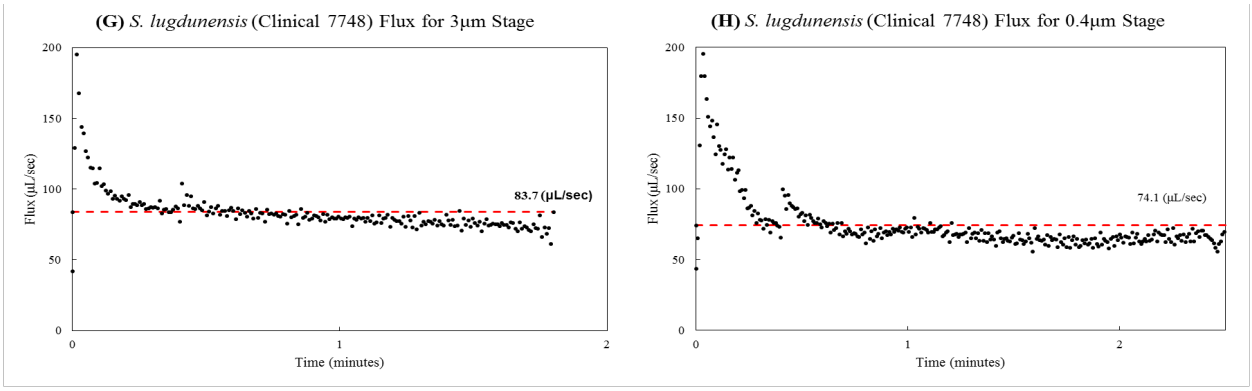

Figure 11: PBC Flux Over Time Across 3µm and 0.4µm filters. We filtered PBCs of *S. epidermidis* (A, B), *S. aureus* (C, D), *E. faecalis* (E, F), and *S. lugdunesis* (G, H) through 3µm (A, C, E, G) and 0.4µm filters (B, D, F, H). We measured the volume of permeate from each filter over time and then calculated and plotted the flux over time. We averaged the flux for each sample, shown in the red dashed line on each graph.

For the 3µm filtration, samples took no longer than 2 minutes to completely filter. Flux decreased steadily and relatively slowly over time for all samples except *E. faecalis*, which increased by about 40µL/s throughout filtration. For the 0.4µm filtration, the flux for all samples decreased rapidly within the first 30 seconds to minute followed by a steady decrease similar to that of the first stage. The flux across the 3µm filter averaged 66.65µL/s for all samples while the flux across the 0.4µm filter averaged 52.75µL/s, demonstrating a higher flux for larger pore sizes.

While processing single aliquots allowed us to characterize flux across the membrane over time, we sought to determine the point at which flux remains constant across the filter membrane. Thus, we performed a stress test for both the 3µm and 0.4µm filter. We used the same setup; however, rather than running one aliquot of PBC, we continued to filter PBCs through the same filter until we observed constant flux across the membrane. The 3µm membrane filtered 63ml over 9.5 minutes while the 0.4µm membrane filtered 58mL over 68.5 minutes (*Figure 12*). We stopped the 0.4µm filtration due to sample and time constraints.

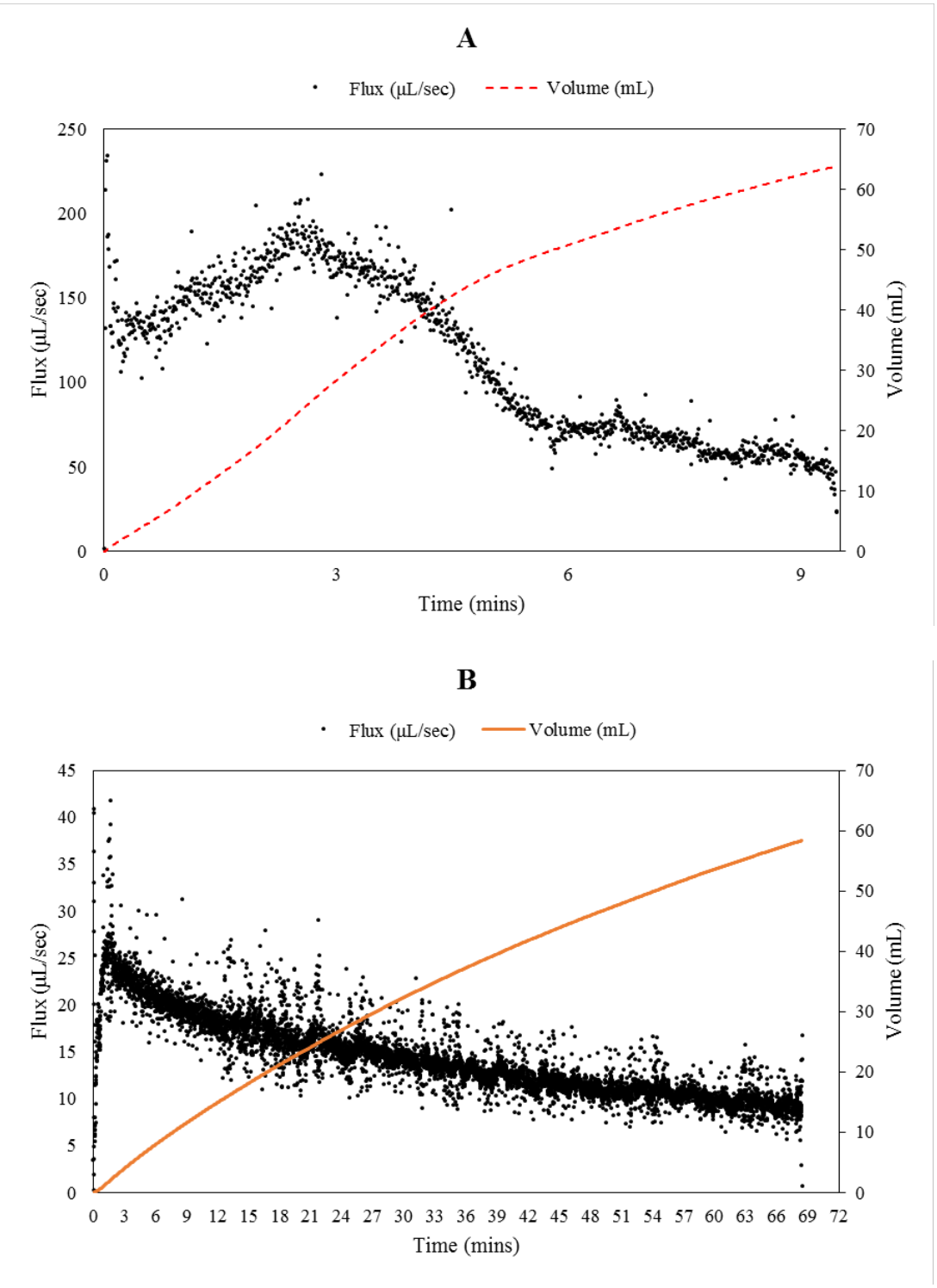

Figure 12: Stress Test of Flux Over Time Across 3µm and 0.4µm Pores. We continued filtering PBCs through the same 3µm (A) and 0.4µm (B) filters in order to observe a point of constant flux. We measured the volume over time (orange line) and then calculated the flux over time. We stopped filtering PBCs through the 0.4µm after 68.5 minutes due to time and sample constraints.

For the 0.4µm filtration, flux increased sharply at the start of processing before starting a slow decline. While the decline remained consistent with the single aliquots we tested, the overall flux throughout the filtration process started at and decreased to a much lower value. This signifies potential buildup of a cake layer that ultimately prevents remaining sample from filtering. The flux during the 3µm filtration increased by about 150µL/s over 3 minutes before starting to decrease. Although this differed from the single aliquot samples, it is possible that the short time period over which we collected that data would not reveal this behavior.

Effect of Increasing Filter Pore Size

After observing increased flux with a larger pore size, we sought to improve bacterial recovery by increasing the first stage filtration pore size from 3µm to 5µm. We processed the thirty bacterial strains grown in PLUS Aerobic media through a filter scheme of 5µm/0.8µm and compared downstream test results to the results of the 3µm/0.4µm filter scheme. Prior to gathering performance data, we quantified red blood cell passage through varying pore sizes in order to determine feasibility and understand the effect of red blood cell passage on future downstream testing performance.

Red Blood Cell Passage. We compared the percent passage of red blood cells from an NBC through a 5µm filter to the percent passage through 3µm, 2 µm, and 1 µm. 34.9% of red blood cells passed through the 5µm filter while 10.2%, 1.4%, and 0.1% passed through the 3µm, 2 µm, and 1 µm filters, respectively (*Figure 13*).

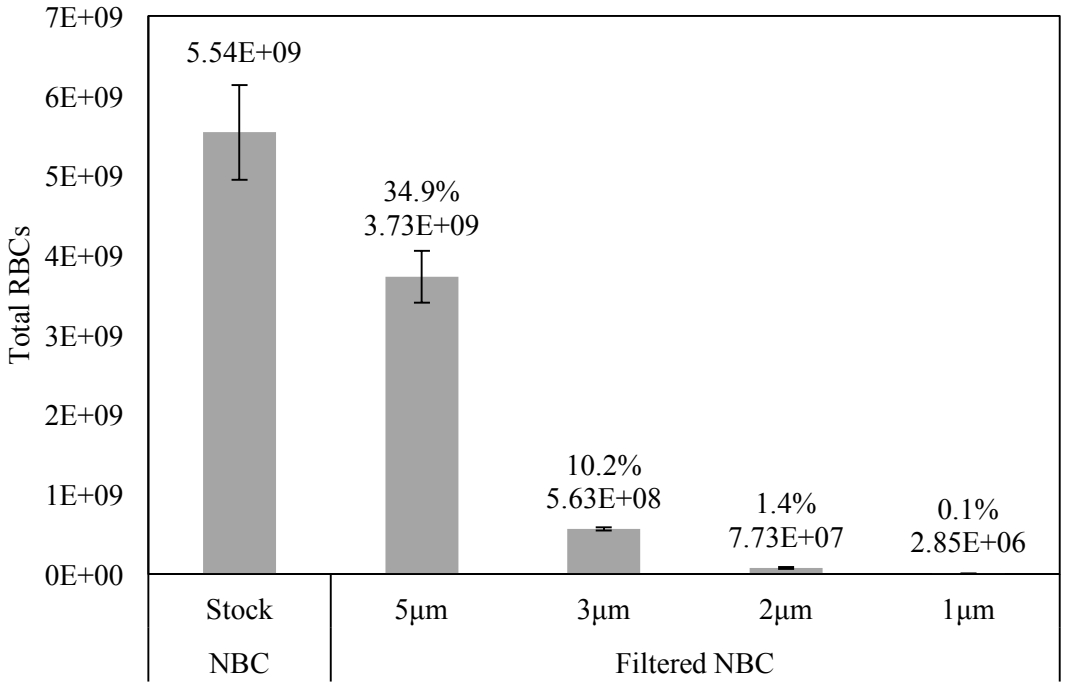

Figure 13: Percent Passage of Red Blood Cells from a Negative Blood Culture through Varying Filter Pore Sizes. We filtered aliquots of a negative blood culture (NBC) through 5µm, 3µm, 2 µm, and 1 µm filters. We quantified red blood cell (RBC) passage using a hemocytometer. We calculated percent passage using the original number of RBCs in the NBC.

Each increase in pore size resulted in about a tenfold increase in total RBC passage. Although the percent passage of RBCs through the 5µm filter was triple the percent passage through the 3µm filter, we moved forward with testing this increase in pore size. The results of this experiment allowed us to determine the effect of increased RBC passage, as well as prioritize maximization of bacterial passage versus minimization of RBC passage.

Recovery of Bacteria. We averaged the plate counts from PLUS Aerobic PBCs processed through a 5µm/0.8µm filtration scheme and compared the results to those processed through the 3µm/0.4µm scheme. For Gram negative bacteria, the 5µm filter recovered an average of 5.71×10^9 CFU versus 6.88×10^9 CFU recovered from the 3µm filter. The 3µm filter recovered more total CFU from the PBC for all Gram negative PBCs (*Figure 14 A*). For Gram positive bacteria, the 5µm filter recovered an average of 2.71×10^9 CFU versus 2.32×10^9 CFU recovered from the 3µm

filter. The larger filter scheme recovered more CFU from the PBCs of *S. aureus*, *S. epidermidis*, and *S. lugdunensis* (*Figure 14 B*).

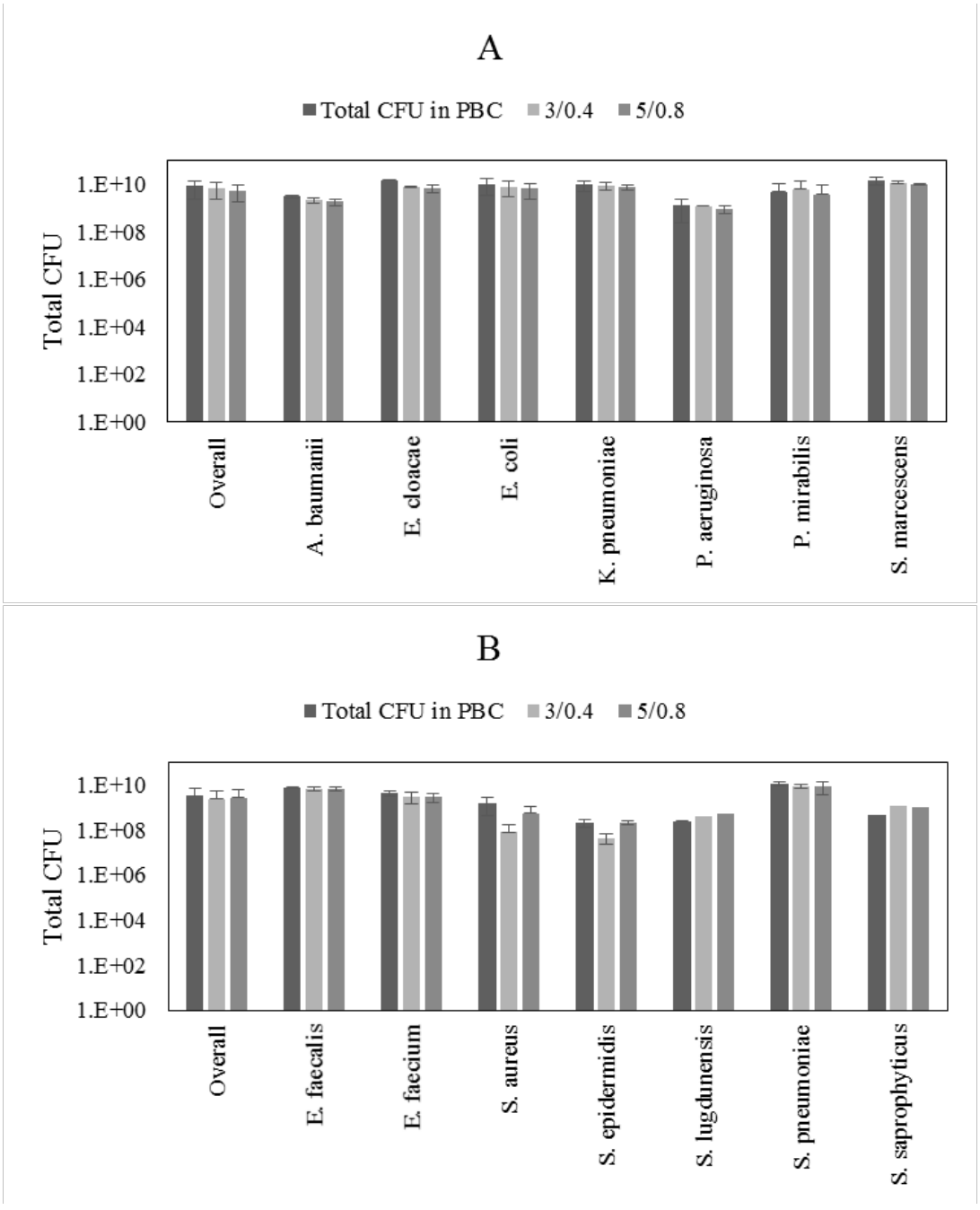

Figure 14: Total CFU in PLUS Aerobic PBCs vs. Outputs from 3.0µm and 5.0µm Filtration Schemes. We processed two aliquots per strain of microorganism, one through a 3µm/0.4µm scheme and one through a 5µm/0.8µm scheme. We averaged plate counts across strains before and after processing. We compared total CFU in the output from each filter scheme to one another and to the original PBC. We plotted these values for Gram negative bacteria (A) and Gram positive bacteria (B).

Overall for Gram negative bacteria, the total CFU recovered from a larger pore size remained relatively the same as a smaller pore size. Gram positive bacteria, specifically *Staphylococci*, saw an increase in total CFU recovered with a larger filter size. We recovered nearly tenfold the number of bacteria from the larger filter compared to the smaller filter ($5.39x10^8$ vs. $7.95x10^7$, respectively), which improved percent recovery from 3.9% to 24.1%. Furthermore, we recovered $5.39x10^8$ CFU of *S. epidermidis* from the larger filter versus $4.42x10^7$ CFU from the smaller filter—a shift from 24.0% to 111.9% recovery (*Figure 15*).

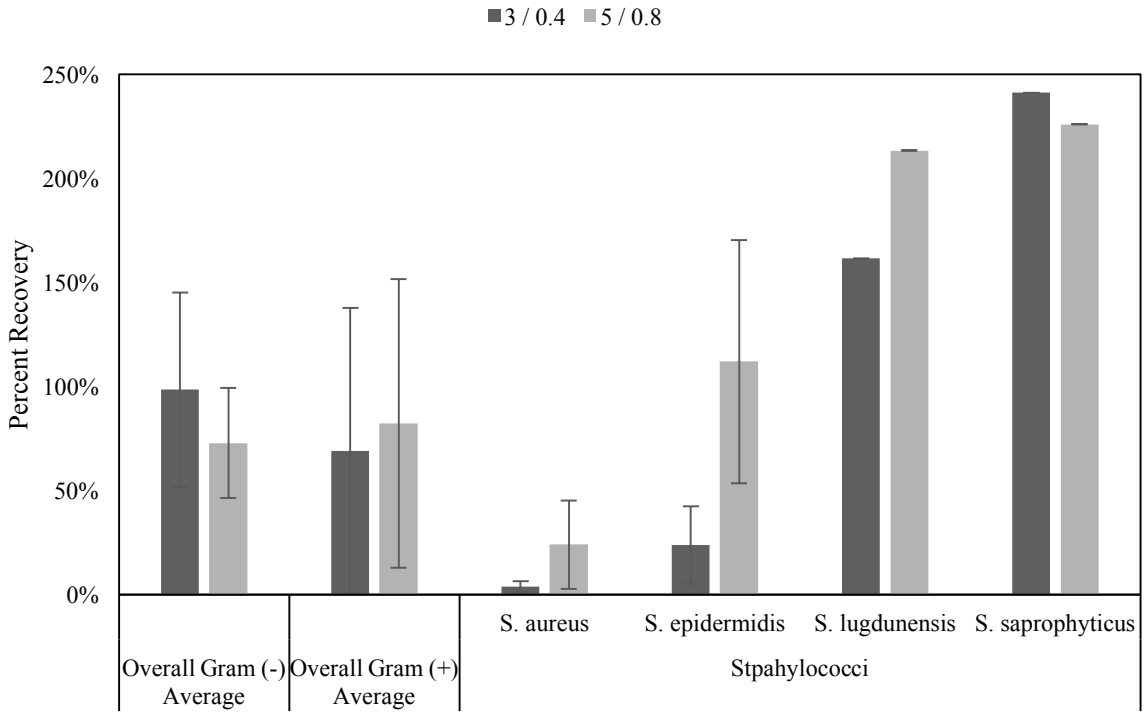

Figure 15: Percent Recovery from PLUS Aerobic PBCs Processed through 3.0µm and 5.0µm Filtration Schemes. We calculated percent recoveries for each strain using the total CFU from the original PBC and outputs. We averaged the percent recoveries across strains of Gram negative and Gram positive organisms, as well as each species of *Staphylococci*. We focused on *Staphylococci* due to the low percent recovery from the original filter size and its inability to generate consistent ID/AST results.

While the percent recovery of Gram negative bacteria decreased overall, the number of total CFU recovered from the larger filter remained much the same as the original filter size. Additionally, previous ID/AST results show that downstream testing with Gram negative outputs are much more

concordant with the reference method than Gram positive bacteria. Since recovery of Gram positive bacteria—and especially *Staphylococci*—increased with a larger pore size, we moved forward with downstream testing in order to determine if more bacteria improve ID/AST results.

Phoenix AST Performance. We used the same reference PBC AST results for samples filtered through both the 3µm and the 5µm schemes. For all Gram negative bacteria, the 5µm scheme yielded nearly equal results as the 3µm scheme, averaging 99.35% of MICs in essential agreement versus 99.14% of MICs for the 3µm (*Table 3*). For Gram positive bacteria, 90.02% of MICs yielded an essential agreement for the 5µm scheme versus 89.09% for the 3µm. While the percent of Gram positive samples with no AST growth remained the same across both filter sizes, the percentages of *S. epidermidis* and *S. pneumoniae* both decreased from 33.66% to 25.19% and 7.14% to 0%, respectively.

Table 3: Phoenix AST Results for PLUS Aerobic PBCs Filtered through 3µm vs. 5µm Schemes.

Organism	# of Strains	3			5		
		Total n	Essential	No AST Growth	Total n	Essential	No AST Growth
Gram Negative	**16**	**463**	**99.14%**	**0.00%**	**463**	**99.35%**	**0.00%**
A. baumanii	2	58	96.55%	0.00%	58	98.28%	0.00%
E. cloacae	2	58	100.00%	0.00%	58	100.00%	0.00%
E. coli	3	87	100.00%	0.00%	87	100.00%	0.00%
K. pneumoniae	3	87	98.85%	0.00%	87	98.85%	0.00%
P. mirabilis	2	58	100.00%	0.00%	58	100.00%	0.00%
P. aeruginosa	2	58	100.00%	0.00%	58	100.00%	0.00%
S. marcescens	2	57	98.25%	0.00%	57	98.25%	0.00%
Gram Positive	**14**	**605**	**89.09%**	**5.95%**	**571**	**90.02%**	**5.95%**
E. faecalis	2	68	95.59%	0.00%	68	95.59%	0.00%
E. faecium	2	102	94.12%	0.00%	102	100.00%	0.00%
S. aureus	4	204	98.04%	0.00%	170	98.24%	0.00%
S. epidermidis	2	101	49.50%	33.66%	135	62.22%	25.19%
S. lugdunensis	1	34	100.00%	0.00%	34	100.00%	0.00%
S. saprophyticus	1	68	100.00%	0.00%	34	100.00%	0.00%
S. pneumoniae	2	28	92.86%	7.14%	28	100.00%	0.00%
Overall Total	**30**	**1068**	**93.45%**	**3.37%**	**1034**	**94.20%**	**3.29%**

Overall, the increase in filter size did not yield significantly more accurate AST results; however, the problematic *S. epidermidis* strains saw an increase in both exact and essential agreements by over 10%. Although 62.2% of MICs remains well below concordant with the reference standard, the corresponding increase in total CFU recovered by switching to a larger filter size signifies that more bacteria aids in accuracy of AST results. Furthermore, an increase in passage of RBCs through the larger filter may contribute to the turbidity of the output sample, impeding growth in certain AST wells and effecting the overall MIC for certain drugs.

MALDI ID Performance. We compared MALDI scores for PLUS Aerobic PBCs filtered through a 3µm scheme versus a 5µm filter scheme. Overall, filtering through a larger pore size yielded more accurate identification of bacteria with 96.77% (n=30) of all samples identifiable to at least the genus level versus 88.89% (n=28) from the 3µm scheme (*Figure 16 A*). Gram negative bacteria remained consistent across both filter sizes, yielding accuracy to the species level for 100% of samples (*Figure 16 B*). Gram positive bacteria yielded at least genus-level identification accuracy for 93.33% (n=14) of samples filtered through the larger pore size versus 80.00% (n=12) of samples filtered through the smaller pores (*Figure 16 C*). Within the Gram positive samples, *E. faecalis*, *E. faecium*, and *S. pneumoniae* yielded 100% identification accuracy to the species level for both filter sizes. For the remaining bacteria (i.e. *Staphylococci*), 87.5% of samples identified at least to the genus level with only one sample (*S. aureus*) yielding no reliable identification whereas 3 samples filtered through the smaller pore size yielded no reliable identification (*Figure 16 D*).

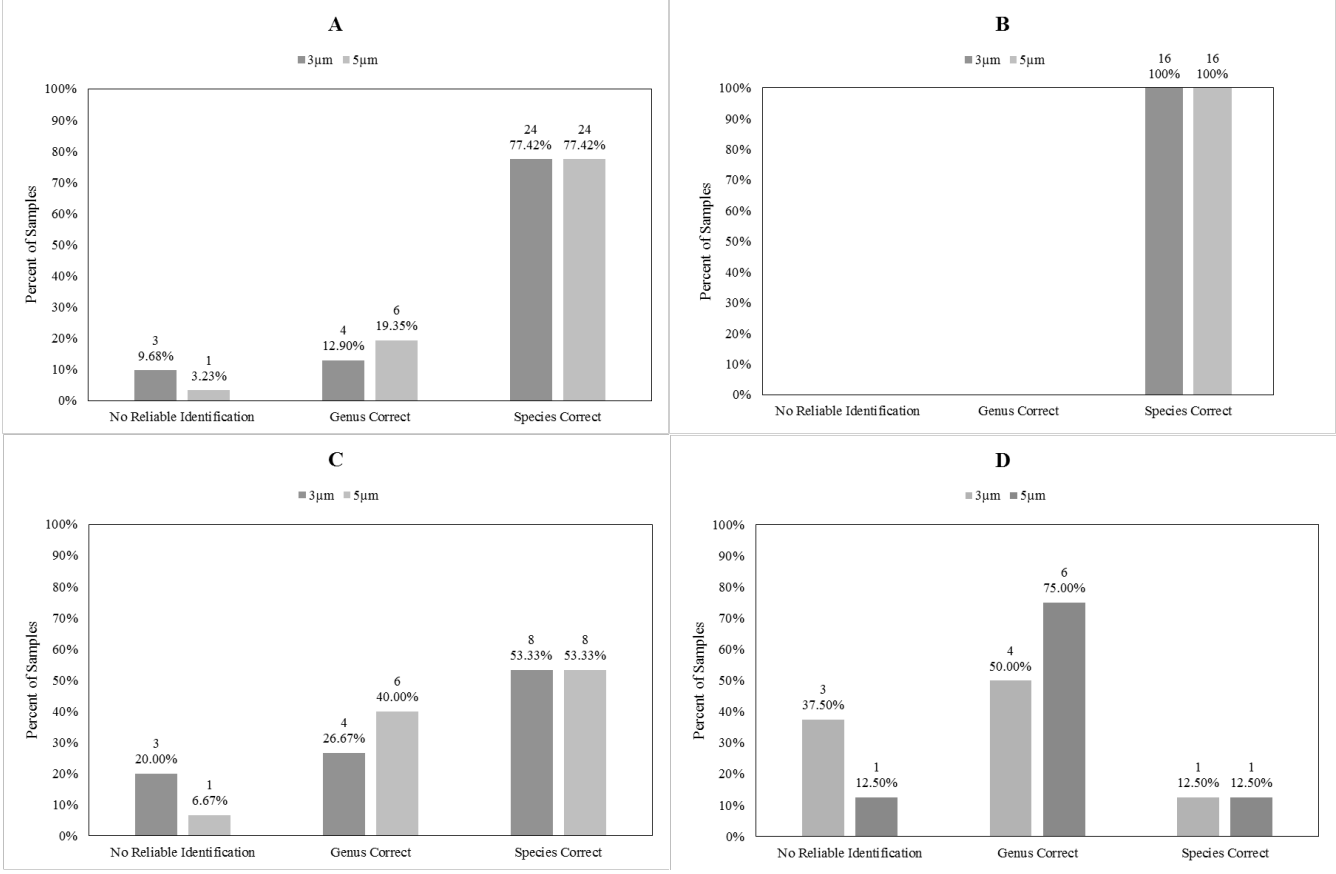

Figure 16: Distribution of MALDI Scores for PLUS Aerobic PBCs filtered through 3µm vs. 5µm Schemes. We compared the accuracy of MALDI identification for samples filtered through a 3µm versus 5µm filter scheme. We grouped scores based upon recommendations from Bruker. We looked at the overall score distribution across all bacteria (**A**) before narrowing the distribution to only Gram negative (**B**) and positive (**C**) bacteria, and finally *Staphylococci* (**D**).

From these results, we see that filtering samples through a larger pore size increases accuracy of identification, most likely due to an increase in bacteria. Moreover, this increase did not affect identification of Gram negative bacteria. This implies that the additional amount of bacterial passage through the filter outweighs any impeding effects of RBC passage. Although increasing filter pore size looks promising, *Staphylococci* strains still propose a challenge for accurate ID/AST results.

DISCUSSION

Although we successfully adjusted processing parameters during the baseline study to generate as accurate results as possible, there remains much room for improvement for PBC

processing. Difficulties yielding accurate results for PBCs grown in lytic media and Gram positive PBCs show that excess blood background and lack of bacteria in the output play key roles in ID/AST results. While the optimal balance between more bacteria and less blood background remains relatively uncertain, our preliminary results suggest that increasing filter pore size yields better ID/AST results.

PBC Processing Workflow

The general workflow for PBC processing remained consistent with its original protocol as it proved relatively robust across media and bacteria types. This being said, we made several adjustments to the workflow depending upon the PBC media type. A major adjustment included pre-filtering of resin beads PLUS Aerobic PBCs, necessitating an extra step in the workflow. Additionally, the material, volume, and timing of the wash step became critical for all media types, but mainly Lytic Anaerobic. Proper application of the washes avoids premature cell lysis and aids sample flow across the TEM to minimize cake buildup. While we easily made these adjustments to our benchtop technology, development of next generation technology must keep in mind and accommodate for the necessary deviations for various media types.

In order to successfully standardize the workflow and eventually automate the system, limits for processing time, wash volume, and the required hands-on time must be defined and remain consistent across all media types. Alternatively, a separate device may be designed for each specialty media types. For instance, a device for PLUS aerobic PBCs that includes an additional filtration system, or a device for Lytic Anaerobic PBCs that includes a higher wash volume. Still, the PBC processing workflow remains relatively straightforward in its current state with capabilities across all media types and most microorganisms.

Baseline Data

As previously mentioned, PBC processing showed robustness across all media types and most microorganisms. This being said, *Staphylococci* yielded problems for all aspects of the baseline study, most likely due to clumping of colonies and subsequent inability to filter. A microfluidic device that physically separates clumps of colonies prior to filtration has potential to increase percent recovery for these strains and collect more bacteria. The number of bacteria required from the output for downstream testing still needs to be defined, but preliminary results showed that more bacteria and higher percent recovery yields better results.

PBC processing yields a variable percent recovery of bacteria from the original PBC, especially across media types. However, a majority of the strains processed yielded substantially high percent recoveries, again with the exception of *Staphylococci*. For most cases that yielded greater than 100% recovery from the PBC, this can be attributed to a lag between the time of the initial plate count and initiation of PBC processing, allowing for further growth. Furthermore, we performed plate counts by hand and while we strived to be as accurate as possible, the margin of error remains very large. Another explanation for generating more CFU in the output than the PBC is the potential of bacterial concentration outweighing any bacterial loss, thus indicating high filter performance.

While percent recovery is important for assessment of filter performance, it can be misleading and a low percent recovery is not necessarily an indicator of poor downstream test results. In cases of low percent recovery, it is important to additionally consider the total CFU in the output. Looking at a low percent recovery with an output CFU on the order of 10^8 or higher tells us that while we do have ample bacteria for downstream testing, the filter is operating inefficiently and warrants the need for further optimization and improvement. Thus, the number

of total CFU in the output tube must also be considered when defining a lower limit for percent recovery and the necessary number of bacteria required for ID/AST.

S. epidermidis remained the single bacterium yielding discordant AST results across all media types. Again, this most likely stemmed from lack of bacteria in the output. This being said, for *S. epidermidis* and other samples yielding concordant, but less than 100% essential agreement, excess blood background in the output may contribute to the turbidity of the sample in AST panels. Since Phoenix AST continuously monitors panel wells for changes in turbidity, a sample with increased turbidity from blood background may not be detected as having any change in turbidity despite growth, thus decreasing the MIC and yielding inaccurate AST results. This potential explanation becomes apparent with lower concordance levels of lytic PBCs, which generally yield discolored outputs. A lower than actual MIC becomes especially problematic in the field when a sample may be called susceptible at a lower than actual concentration of drug, leading to ineffective killing of the bacteria. While this warrants further investigation on how to improve AST results, our baseline results were concordant with the reference method, again with the exception of *S. epidermidis*.

Accuracy of MALDI Identification

Throughout all of our testing, MALDI proved to be the most difficult and inconsistent aspect. Poor accuracy from Lytic Anaerobic, *Staphylococci*, and other Gram positive PBCs implicate that both residual blood background and lack of bacteria impede accurate ID results. Even with adjustments to our processing workflow to account for these factors, difficulties with ID remained.

The ID results from increasing the filter pore size (*Figure 16*) showed that more CFU recovered and yielded a more accurate ID. Additionally, we found that outputs that yielded less than 10^8 total CFU consistently yielded a score classified as "no reliable ID;" however, several samples grown in Standard Aerobic (e.g. *S. leggedness*, *E. faecium*) and Lytic Anaerobic (e.g. *E. coli*, *K. pneumoniae*) media yielded $6x10^8$ total CFU and also scored "no reliable ID." Thus, while we can postulate that an increase in bacteria increases the accuracy of ID, we must fully understand the behavior of samples with ample bacteria that yield no reliable ID.

Lack of accurate ID in samples with both low and high recovery rates may arise from limitations of our MALDI sample preparation. Previous work demonstrates that identification of Gram positive bacteria improves with extraction of proteins from bacterial colonies prior to application to the target plate[15, 16]. Throughout the entirety of this project, we applied bacterial colonies or PBC outputs directly to the target plate before using formic acid to disrupt cell membranes to release proteins. This allowed for a fast, simple protocol; however, improper extraction of proteins leads to a lack of analytes and insufficient generation of peaks. Thus, while increasing the number of CFU in the outputs may inherently aid in generating a more accurate peak, a larger number of bacteria may not be a necessary input to MALDI if we perform a more thorough extraction from the sample.

Inaccurate IDs may also stem from diminishment of target peaks due to excess blood background and contaminants. Throughout the entirety of the baseline study, we saw that samples with visible amounts of blood background yielded poor MALDI results, if any at all. If residual blood proteins or even excess salts from saline washes remain at levels similar to that of the recovered bacteria, the contaminant peaks interfere with definition and identification of the target peaks. However, increasing the TEM pore size increases passage of both bacteria and RBCs, but

the additional blood background did not seem to hinder MALDI accuracy. Thus, the effect of blood background contamination must be further investigated.

Flux Across the TEM and Cake Layer Formation

Based upon a decrease in flux across the TEM over time, we hypothesize that cake layer formation occurs. This becomes more apparent at smaller pore sizes, which corresponds to ease of clogging. Since this portion of the study aimed to identify potential causes of poor filtration for Gram positive bacteria, we only characterized the flux of Gram positive strains. While Gram negative bacteria generally perform well with no alterations in filtration, we still must characterize the flux across the TEM for these strains in order to get the complete picture of what occurs at the membrane.

A decrease in flux and subsequently low bacterial recovery implies hindrance at the TEM, but may be due to a lack of available sample in the filtrate rather than cake layer buildup. In order to prove cake layer buildup, a scanning-electron micrograph of the actual filter must be taken to observe microscale cake formation and clogging of pores. Meanwhile, collection and plating of the permeate from several consecutive time points will allow observation of the actual change in number of bacteria collected over time. In addition to aiding characterization of filtration, measuring the concentration of bacteria in permeate over time may allow for significant decrease in processing time. If all bacteria get collected after one minute and no additional bacteria filters after that point, filtration time can be reduced from approximately three minutes.

Effect of Increasing Pore Size

In a first attempt to improve flux and bacterial recovery, we increased the pore size. With this, we saw increased percent recovery of Gram positive strains, most likely due to their ability

to fit through the pores despite clumping. We did not see any significant improvement for Gram negative strains, but more importantly we did not observe a decrease in ID/AST accuracy for those strains. This was originally a concern as we were uncertain if an increase in RBC passage would negatively impact downstream testing. While results proved that increasing the pore size improves the percent recovery and ID/AST results for Gram positive bacteria, we tested a limited sample size. In order to get more definitive answers and to implement this larger pore size into the PBC processing workflow, the study must be expanded across Standard Aerobic and Lytic Anaerobic media.

Based upon the RBC passage through a larger pore size and subsequent capability of the output to yield accurate ID/AST results, it becomes apparent that the need for more bacteria outweighs the interference of blood background. A large amount of outputs from the larger pore size contained discoloration similar to the outputs of lytic media, indicating excess blood background. While we originally hypothesized that this would interfere mostly with MALDI ID results, it was not the case and we yielded more accurate IDs. With this, we must further define the maximum pore size or, more generally, the optimal ratio of bacterial to RBC passage that allows for accurate ID/AST.

CONCLUSIONS AND RECOMMENDATIONS

PBC processing allows for separation of bacteria from blood cultures, yielding an input for accurate ID/AST results and ultimately decreasing the time to confirmatory bloodstream infection diagnosis by 18 hours. Preliminary baseline testing demonstrates that the technology is capable of processing blood cultures containing a wide variety of bacteria grown in various media types. While there remain necessary adjustments depending on the media and microorganism type, these

are relatively simple and easily applicable to an automated technology. This being said, the technology requires further development in order to fully optimize processing, especially for problematic *Staphylococci* strains. Moreover, understanding the limits of detection of the output in both MALDI ID and Phoenix AST is key to defining performance parameters for this development.

There are several ways to improve processing performance and better prepare the final output for downstream testing. In order to minimize cake layer formation and maximize bacterial recovery, the physical geometry of the filter must be optimized. Simply increasing the size of the filter would create more surface area for sample flow and thus minimize pore clogging and cake filtration; however, the dimensions must remain feasibly in relation to the final disposable design. Alternatively, increasing the channel height would also increase the area through which the sample flows and thus decrease cake buildup. Once the geometry is optimized, both the flowrate of the peristaltic pump and pressure of the vacuum pump must be optimized in order to further maximize bacterial recovery.

After alteration of the actual filter, it is important to conduct another baseline study and compare the results to those aforementioned. This will allow confirmation of optimization and determine if bacterial recovery is improved. Definition for the necessary amount of output for MALDI ID and Phoenix AST would aid in qualification of the new baseline results. Furthermore, analyzing MALDI itself in order to determine its tolerance of blood background would allow for an increase in the TEM pore size. With complete optimization of the physical filtration system and further definition of requirements for ID/AST, PBC processing can be implemented into an automated device. This will significantly improve the diagnosis of bloodstream infections and ultimately improve the outcomes of sepsis patients.

Chapter 2: Characterization of Fluorescence-Based Oxygen Depletion Sensor Formulations for Conversion from Glass to Polycarbonate Blood Culture Bottles

ABSTRACT

The diagnostic workflow for a bloodstream infection begins with a blood draw into a culture bottle, which must then be transported to a lab for incubation in an automated instrument that monitors bacterial growth. Blood culture systems utilized glass collection bottles when they came on the market prior to the year 2000. However, transporting glass bottles creates safety hazards and high disposal costs, and over time there has been a trend toward centralized diagnostic labs that require inter-facility transport of incubated bottles. Conversion of blood culture bottles to a lightweight plastic allows for easier transportation, more economical disposal, and eliminates the hazards of broken glass and spills. This being said, adhesion of the fluorescence-based sensors necessary for detection of microorganism growth in a blood culture bottle remains poor as the sensors detach from the plastic bottle base. This detachment prevents detection of growth since blood culture components get between the sensor's fluorescence indicator and the instrument's photodetector, interfering with growth monitoring. Previous development efforts selected a promising adhesion promoter for proper stabilization of the sensor within BD's plastic blood culture bottle; however, full characterization of the adhesion levels and signal ranges of new sensor formulations remain unclear.

In order to define adhesion levels of two finalized sensor formulations—Sensor A and Sensor B—we developed a quantitative scale to minimize subjectivity of the previously established qualitative adhesion assay. This allowed us to select plasma treatment conditions for preparation of the polycarbonate bottles at the research and development site. From this, we prepared a pilot-scale evaluation of the adhesion level and dynamic range of Sensor A versus Sensor B using bottles plasma treated at the research and development site, as well as bottles plasma treated at the manufacturing site. Only Sensor A in polycarbonate bottles plasma treated at

the manufacturing site yielded adhesion similar the current product for sale; however, we found a higher baseline signal reading and thus narrower dynamic range for Sensor A. We selected only Sensor A to move forward with the scale-up process due to failure of Sensor B to adhere to the bottle. Biological testing of Sensor A will determine the effects of a smaller dynamic range on sensitivity of growth detection. Further development of alternate formulations is recommended should Sensor A yield performance issues during scale up. With this, full conversion of blood culture bottles to polycarbonate bottles will improve safety and ease of disposal, ultimately improving the diagnosis of blood stream infections.

INTRODUCTION

While conversion of blood collection tubes from glass to plastic has been available for over ten years, plastic blood culture bottles for major automated systems only recently became available. Furthermore, many laboratories were slow to convert to plastic collection tubes due to various barriers[18]. With an increasing incidence of sepsis and larger quantities of blood cultures being processed, nurses and laboratory workers are increasingly at risk for exposure to blood borne pathogens. Specifically, the use of pneumatic tube systems that shuttle specimen vessels from collection points to labs can cause glass bottles to break and leak contaminated material. Conversion to plastic, shatterproof culture bottles not only eliminates this risk, but it produces significantly less medical waste as plastic bottles are smaller and weigh less than glass.

While conversion to plastic culture bottles improves safety and decreases disposal costs, the performance of the bottle's sensor must be kept in mind. Glass inherently has a high surface energy, and thus the fluorescence-based sensors remain attached to the surface; however, polycarbonate plastic bottles possess a relatively low surface energy and thus their sensors require an inert adhesion promoter. Beginning in July 2016, BD began conversion to plastic for blood culture bottles containing fluorescence-based sensors that detect microorganism growth via carbon dioxide production[19-21]. While the adhesion promoter in these bottles successfully holds the sensor in place, conversion of culture bottles that detect oxygen depletion (i.e. culture bottles for detection of mycobacteria and fungi) yielded displacement of the sensor from the bottle with the suggested adhesion promoter. If this displacement occurs during incubation of the culture, growth detection will be prevented as blood and other culture components will interfere with detection of fluorescence changes.

This project aimed to characterize the adhesion strength of two different formulations for the oxygen depletion sensor, as well as determine the sensor formulations' effects on detection signal range. We first developed a scale in order to quantify adhesion and make comparison of the formulations more straightforward. We then compared the adhesion and signal levels of the two formulations to the current glass product for sale in order to select a formulation for biological verification testing and eventual scale up for manufacturing.

BACKGROUND

The workflow of an automated blood culture system remains relatively straightforward, beginning with a blood draw into the culture bottle, transport to an automated culture instrument (e.g. BACTEC) for incubation, and then removal from the instrument after detection. Yet despite the workflow's simplicity, pre- and post-incubation steps often require transport and disposal of large numbers of blood culture bottles to and from the laboratory. With heavy loads of glass bottles filled with often contaminated blood, it creates large potential for glass breakage, leakage of blood borne pathogens, and ultimately the delay of blood stream infection diagnosis. This warrants conversion of blood culture bottles from glass to a lighter material like polycarbonate, improving the workflow for operators and creating a safer environment for hospitals and labs. Differences in the surface chemistry of glass and plastics necessitates investigation of the bottles' growth detection sensors in order to ensure proper performance with this conversion.

Signal Detection with BACTEC Automated Blood Culture Systems

The BACTEC system exploits fluorescence to detect the growth of bacteria in a blood culture. All BACTEC blood culture bottles contain a fluorescence-based, disk-shaped silicone sensor at the base of the bottle. Each sensor contains a fluorescence indicator that reacts with the metabolites of growing bacteria to detect either an increase in carbon dioxide or a decrease in

oxygen. Light emitting diodes (LED) excite the indicator, which then emits fluorescence proportional to the amount of metabolite present in the culture[22]. Photo detectors in the BACTEC instrument continuously measure emission levels that are interpreted by pre-existing kinetic algorithms. These algorithms analyze emission levels and generate proportional voltage signals, which are used to flag a culture as positive based upon the rate of change in signal.

For the purpose of this project, we focused on sensors that detect oxygen depletion. This sensor, in combination with the blood culture bottle medium, is critical for the detection of slow growing microorganisms such as mycobacteria and fungi. Two components of the sensor formulation—Component 1 and Component 2—are essential for detection. Component 1 is a pigment molecule that remains embedded in the main polymer network of the sensor, while Component 2 serves as the fluorescence indicator and remains flush against the base of the bottle. In order to maximize sensitivity of detection, Component 1 reflects excitation light from the LED back onto Component 2 and emission light from Component 2 towards the photodetector. The presence of oxygen quenches emission from Component 2, and thus a low fluorescence output from the sensor is initially detected[23]. As microorganisms grow they consume the oxygen present in the bottle, yielding an increase in signal as oxygen depletion occurs.

In order to assess the sensor's ability to detect oxygen or carbon dioxide changes, the dynamic range of the computer-generated voltage signal is calculated using the following equation:

$$\text{Dynamic Range} = \frac{\text{(Maximum Voltage)-(Baseline Voltage)}}{\text{Baseline Voltage}} \times 100\% \qquad \text{[Equation 1]}$$

Since the target microorganisms of the oxygen depletion sensor may not grow to detection level for up to six weeks, a large dynamic signal range is necessary to ensure precise growth detection and avoid false positivity.

Sensor Formulation Components

Although the detailed chemistry of the sensor remains proprietary and beyond the scope of this project, knowledge of the main components is important for understanding changes in adhesion and dynamic range across formulations. Each formulation is comprised of three main structural components: (1) a silicone base polymer, which makes up a majority of the formulation; (2) a cross-linker to create the polymeric network of the sensor; and (3) an adhesion promoter that bonds to both the polycarbonate and the base polymer in order to adhere the sensor to the bottle. As previously mentioned, the sensors also contain two components necessary for growth detection. When all components are mixed together the materials remain in a viscous yet relatively thick liquid state. Preparation of bottles requires a five-hour minimum settling time immediately after dispensing the formulations into the bottle. This allows the fluorescence indicator (Component 2) to settle to the base of the bottle in order to maximize fluorescence detection.

Once the components settle, they must be polymerized. With application of heat, three main reactions occur: (1) cross-linking of the base polymer; (2) linking of the adhesion promoter to the polycarbonate bottle; and (3) linking of the adhesion promoter to the base polymer network. Component 1 also becomes embedded in the main polymeric network while Component 2 remains flush against the bottom of the bottle, yielding two distinct layers within the sensor. This process occurs in an oven and results in a rubbery, disk-shaped sensor that ideally stays put at the bottom of the bottle.

Plasma Treatment for Improved Adhesion

While polycarbonate is an ideal material for blood culture bottles due to its strength and lightweight nature, adhesion to its surface becomes difficult due to its relatively low surface energy

and potential contaminants (e.g. oils, dirt, etc.). Plasma treatment serves to improve adhesion by eliminating contaminants and increasing the surface oxygen content in order to promote chemical bonding[24]. In order to treat surfaces with plasma, the materials are placed in a chamber, which is evacuated to create a vacuum[25]. Air or another gas then flows into the chamber at low pressure before applying a high voltage across it to promote ionization and creation of free radicals on the surface of the polycarbonate. These free radicals react with the oxygen in the plasma to increase the surface energy of the polycarbonate by forming functional groups such as carboxyl, hydroxyl, and carbonyl groups[26]. At high enough power and/or long enough treatment times, plasma treatment also has the ability to etch the surface of the material being treated, improving adhesion through physical alteration.

Previous Work for Conversion of Culture Bottles from Glass to Plastic

BD previously conducted several experiments in order to incorporate an adhesion promoter into the current glass oxygen depletion sensor formulation for conversion from glass to plastic blood culture bottles. Based upon recommendations from chemistry experts, one adhesion promoter was tested. After varying the ratios of adhesion promoter and other sensor components, two formulations—Sensor A and Sensor B—were selected based upon adhesion and signal performances. A plasma treatment study was also conducted in order to determine the optimal plasma treatment conditions for manufacturing. This yielded optimal manufacturing conditions of 150W applied for 20 seconds.

Detailed characterization of the adhesion and signal levels for both Sensor A and Sensor B remained unknown. Thus, determination of the adhesion levels and dynamic ranges of signal for each formulation is necessary before scaling up for verification of growth detection performance, selection of a final formulation, and scale-up to manufacturing.

EXPERIMENTAL METHODS

The adhesion promoter of a sensor is critical for its stabilization within the culture bottle. It ensures that growth detection will not be affected by displacement of the sensor. Higher levels of adhesion promoter should theoretically yield stronger attachment; however, it is important to characterize any effects of increased adhesion promoter on the dynamic range of the sensor's fluorescence signal and sensitivity to growth detection. Furthermore, an economical decision must be made in order to maintain efficient manufacturing. We first developed a quantitative scale to measure the level of adhesion of a sensor to a polycarbonate bottle. We then performed a preliminary adhesion study on Sensor A versus Sensor B to confirm the feasibility of both formulations. From this, we prepared a pilot scale batch to compare the adhesion and signal levels of Sensor A versus Sensor B in polycarbonate bottles treated at the research & development site versus at the manufacturing site. This allowed us to select optimal conditions for scale-up biological testing, which will ultimately determine which formulation goes to market.

Overview of Workflow

For each step of this project, we followed the same workflow for sample preparation and downstream testing (*Figure 17*).

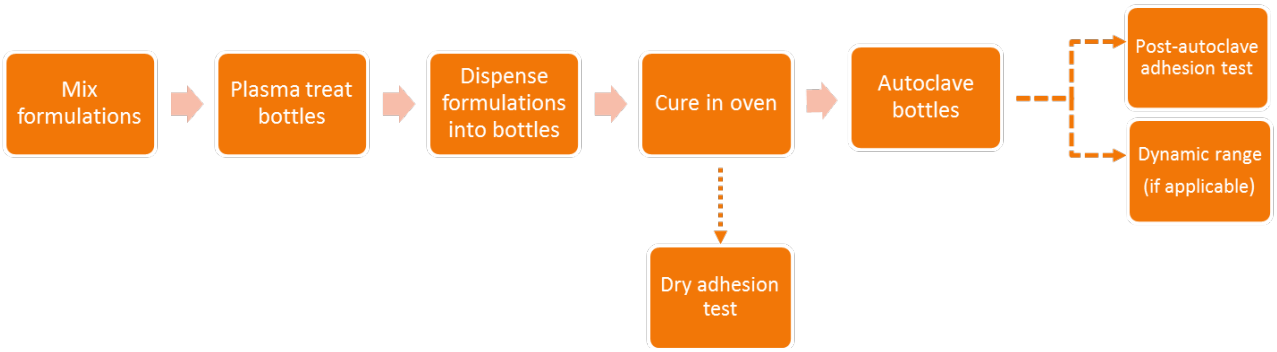

Figure 17: Workflow for Sample Preparation and Downstream Performance Testing. Preparation of samples began with mixture of sensor formulations, which are viscous and mixed both by hand and by an electric mixer. Empty polycarbonate bottles were plasma treated and the sensor formulations were dispensed into the bottles. After dispensing, the bottles were held for five hours to allow the fluorescent dye to settle to the bottom of the bottles before

curing in an oven. A dry adhesion test was performed on cured bottles. 20mL of DI water were added to the remaining bottles, which were capped and autoclaved. Post-autoclave adhesion and dynamic range tests were performed on the autoclaved bottles.

Sensor Formulations

We used previously developed sensor formulations throughout the entirety of this project. Our two formulations, A and B, differed only in the amount of adhesion promoter, with Sensor A containing twice the amount of adhesion promoter as Sensor B. After weighing the sensor materials, we mixed each formulation using an IKA Eurostar 60 digital mixer and dispensed 3mL of the specified formulation into plasma-treated polycarbonate bottles.

Curing Program for Sensors

We used an oven to apply heat to the sensor formulations, initiating polymerization and adhesion of the sensors to the polycarbonate bottles. Herein, we refer to this process as curing. We used the same curing program for every sensor tested. The program took five hours in total and included an increase in temperature from room temperature to 100°C over one hour, followed by a four hour hold at 100°C before decreasing back down to room temperature.

Dynamic Range Testing

We used a BACTEC 9240 to collect signal readings from our samples. In order to calculate dynamic range, we first collected baseline readings by placing autoclaved, decanted, and uncapped bottles in the BACTEC instrument and allowing the signal to stabilize. After five hours, we removed and capped the bottles before purging each bottle with nitrogen gas for one minute. This purge essentially quenched the fluorescence sensor and the subsequent reading served as the upper threshold of the sensor signal. In order to collect this reading, we reloaded the bottles into the BACTEC instrument, paying careful attention to place them in the same rack position at the same

orientation. We allowed the sensors to stabilize again for five hours. We calculated dynamic range using the baseline and nitrogen purge readings (see *Appendix 2* for sample calculation).

Scrape Test for Adhesion

In order to measure adhesion levels of the sensor to the polycarbonate bottle, we used a flathead screwdriver to scrape the sensor from the surface of the bottle. Proper adhesion can be visualized by a leftover residue on the bottom of the bottle, even after scraping away a majority of the sensor. We continued scraping the sensor until most of it came off of the bottle so that we could get an accurate depiction of where the sensor bonded to the bottle, if at all.

We tested adhesion levels both before and after autoclave. The pre-autoclave scrape test allowed us to set a baseline for adhesion. Post-autoclave testing allowed us to determine the effects of autoclaving on adhesion levels, and, most importantly, qualify the final adhesion of the sensor since the final products are autoclaved. While this method allowed us to visualize whether or not the sensor adhered to the bottle, it remained a very qualitative method of assessment and warranted a more quantitative approach for assessment.

Quantification of Adhesion Effectiveness

We prepared 16 replicates for eight different sensor formulations, referred to as conditions. We dispensed formulations into polycarbonate bottles plasma treated for 180 seconds and cured the bottles as per the general protocol. For both pre- and post-autoclave scrape tests, we used the following scale to quantify the level of adhesion for each replicate:

Table 4: Quantitative Scale of Adhesion Level.

Level of Adhesion	Description	Example*
9	Comparable to the current polycarbonate bottle containing the CO_2 sensor, which is known as the "gold standard"; relatively difficult to scrape off; leftover residue is thick and patchy, and covers entire bottom and sides	
6	Substantial amount of residue is visible, but not as much or as difficult to scrape as a level 9; residue present on both bottom and sides of the bottle	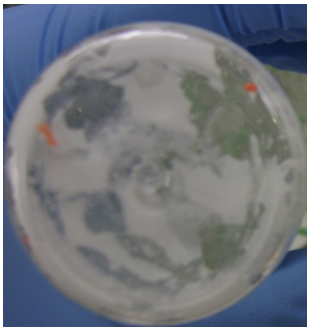
3	Minimal bonding to only one part of the bottle; residue only on sides of the bottle where the sensor attaches, or a small amount on the bottom of the bottle; large patches of no residue	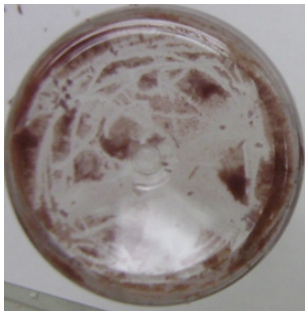
0	No bonding; sensor comes off clean with no residue on the bottom or sides	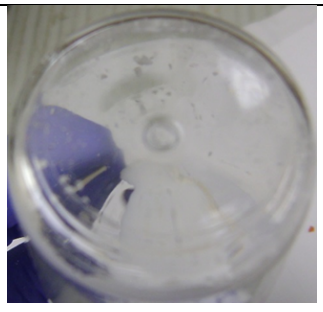

*Note: Pictures of examples are scrape test results of experiments unrelated to this project. Variations of sensor and residue color stems from the components of the particular condition, and are unrelated to adhesion.

Definition of Acceptable Plasma Treatment Level

We plasma treated polycarbonate bottles at increasing lengths of time. For each length of time, we dispensed 3mL of Sensor A into the specified number of bottles, and 3mL of Sensor B into the specified number of bottles (*Table 5*).

Table 5: Bottle Conditions for Assessment of Plasma Treatment Levels.

Formulation	Plasma Treatment Time (s)	Number of Bottles
Sensor A	60	5
	90	5
	180	10
Sensor B	60	10
	90	10
	180	10

We tested adhesion levels for each condition both before and after autoclave. This allowed us to confirm feasibility of each formulation, as well as determine the necessary length of plasma treatment at the R&D site moving forward for scale-up.

Pilot Scale Evaluation

In order to confirm previous findings on a larger scale and perform preliminary testing before scale-up, we compared adhesion levels and dynamic ranges of four different conditions (*Table 6*).

Table 6: Bottle Conditions for Pilot Scale Adhesion and Dynamic Range Assessment.

Formulation	Plasma Treatment Location and Parameters	Replicates
Sensor A	Cayey, Puerto Rico 20s at 150W	35
	Sparks, MD 60s at 500W	35
Sensor B	Cayey, Puerto Rico 20s at 150W	35
	Sparks, MD 60s at 500W	35

After curing, we scrape tested 10 bottles from each condition in order to quantify initial adhesion levels. After autoclaving the remaining bottles, we scrape tested another 10 from each condition in order to quantify the final adhesion level. We then performed dynamic range on the remaining 15 bottles from each condition.

RESULTS

Due to the subjective nature of the scrape test, we faced difficulties quantifying sensor adhesion as one of four levels. Thus, we developed a more robust method for calling adhesion acceptable or unacceptable. From this, we defined a feasible length of plasma treatment time for bottles prepared at the R&D site in Sparks, MD. While longer plasma treatment yielded better adhesion for both sensors, the feasible treatment time for manufacturing limited our selection to a treatment time for which only Sensor A yielded acceptable adhesion. From pilot scale testing, we further found that only Sensor A in bottles plasma treated at the manufacturing site yielded acceptable adhesion. This being said, we found that the increase of adhesion promoter in Sensor A narrows the dynamic range of voltage signal. Despite the smaller dynamic range compared to both Sensor B and the current glass product for sale, we selected only Sensor A to move forward in the scale-up process and toward production.

Quantification of Adhesion Effectiveness

For this experiment, we aimed to assess the robustness of the four-level adhesion quantification scale. We were concerned with the ease of assigning an adhesion level rather than the actual adhesion levels of each condition, and thus will not go into detail about the physical description of the adhesion. We assigned adhesion levels to each of the eight replicates within each condition both pre- and post-autoclave. Across all eight conditions pre-autoclave, half of the

samples yielded a score of 6 while the other half yielded a score of 9 (*Figure 19 A*). Post-autoclave, 51 samples yielded a score of 6 while the remaining 13 samples yielded a 9 (*Figure 19 B*).

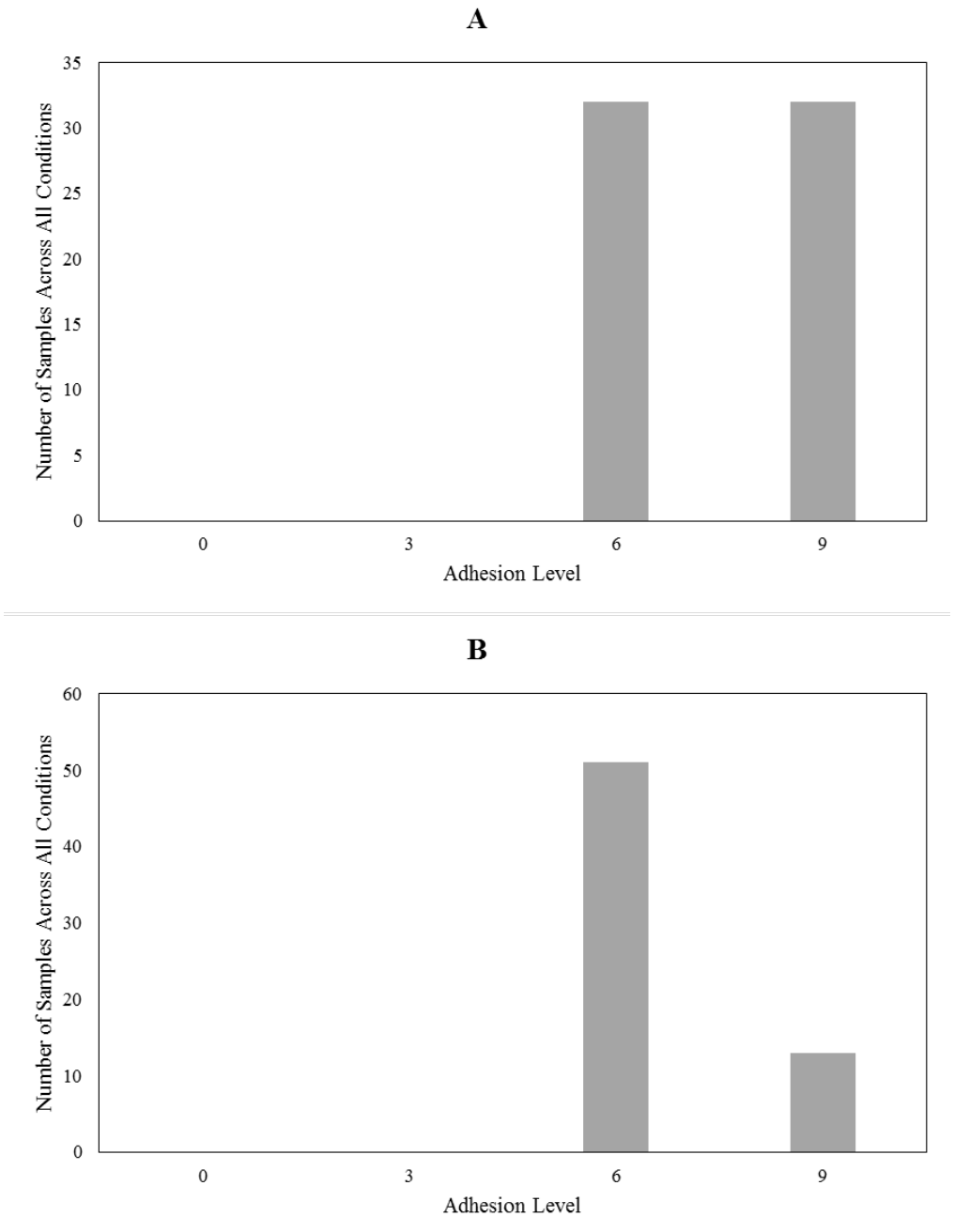

Figure 19: Distribution of Adhesion Levels. We assigned each replicate a level of adhesion both pre-autoclave (A) and post-autoclave (B).

While we assigned an adhesion level to each sample, this assignment remained very subjective. The results from this experiment yielded what we considered acceptable adhesion across all conditions and replicates, making it difficult to decipher between a "6" and a "9" despite the descriptions we developed for each level. This meant that placing the intermediate samples into one level or the other was based largely upon personal experience with the scrape test. This being said, we developed a binary quantification scale in order to avoid further subjectivity as much as possible and make selecting quality samples easier. This binary scale quantifies a sample as 0 or 1, with 0 yielding low or no adhesion and 1 yielding full or partial, thick residue. In other words, we moved towards a scale that qualified a formulation as passing (1) or failing (0) the scrape test.

From the original adhesion level scale, we found (with one exception) no bottle to bottle variability across one condition. For the pre-autoclave scrape test, all samples within the same condition yielded the same level of adhesion (*Figure 20 A*). For post-autoclave, we yielded the same consistency with the exception of condition 4, which yielded 5 samples at an adhesion level of 9 and 3 at a level of 6 (*Figure 20 B,* red box).

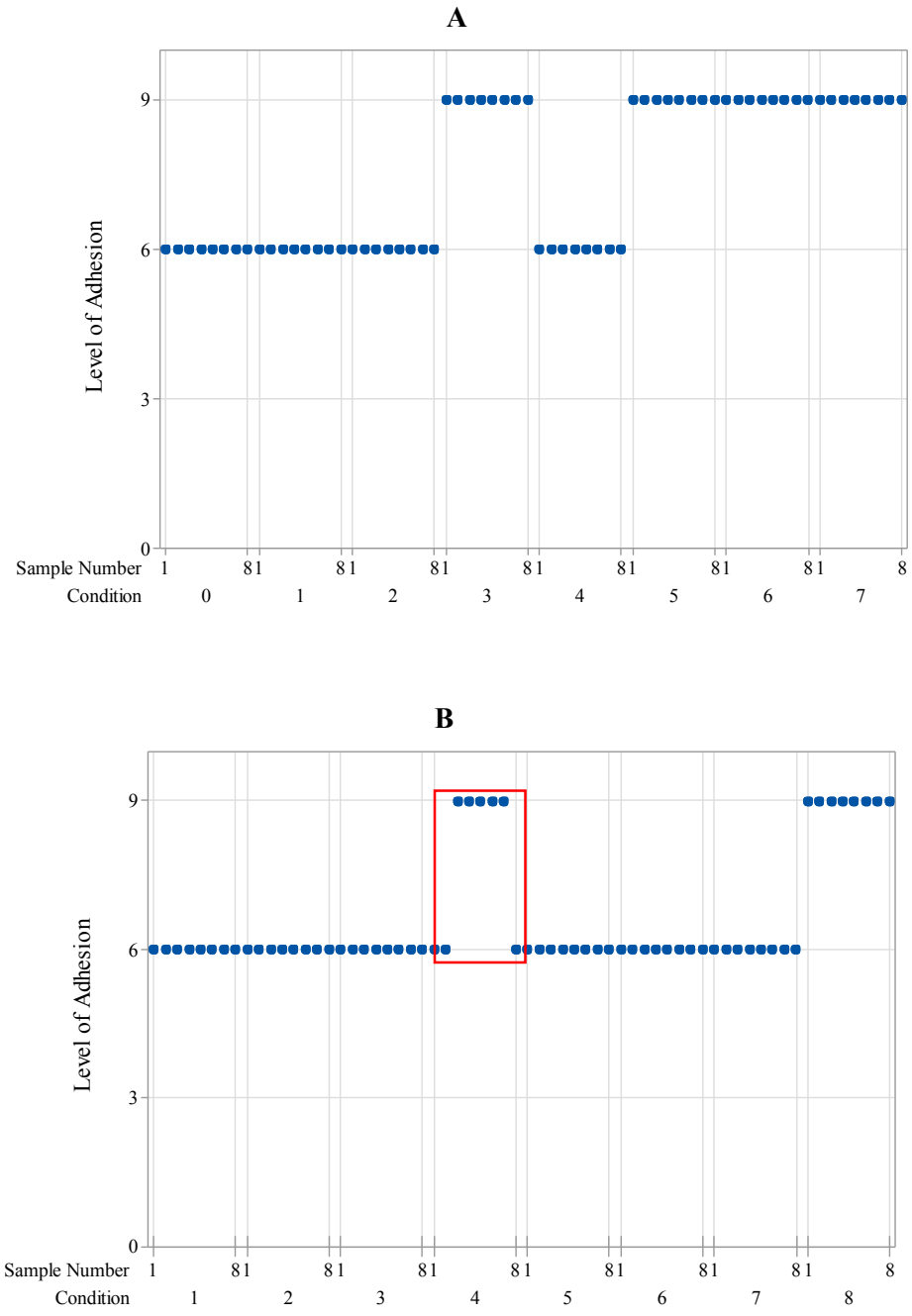

Figure 20: Bottle Adhesion Variability. We assessed the variability of adhesion across replicates within the same condition. We tested adhesion pre-autoclave (A) and post-autoclave (B). We tested eight replicates for each of the eight conditions. Each blue dot represents one replicate. The red box in (B) highlights the samples of condition 4, which was the only condition that showed any variation across its samples.

The relative inconsistency of the post-autoclave condition 4 adhesion can be attributed to the subjectivity of the scrape test. As previously mentioned, the difference between calling adhesion level 9 versus level 6 often proved very difficult if samples laid between the two define descriptions. This being said, this experiment allowed us to confirm low to no sample variability across a condition.

Definition of Necessary Level of Plasma Treatment

We scrape tested a portion of Sensor A and Sensor B samples both pre- and post-autoclave. We are always more concerned with the post-autoclave results and generally used the pre-autoclave results in order to further understand what may cause failure of adherence. Sensor A dispensed into bottles plasma treated for 60 seconds passed the adhesion test pre-autoclave (*Figure 21, top*), but autoclave noticeably decreased the adhesion (*Figure 22, top*). Still, we observed slight residue from this condition. Sensor B on the other hand yielded adhesion only on the sides of 60 second-treated bottles with the remaining portion detaching cleanly from the bottle, thus failing the adhesion test. At 90 seconds of plasma treatment, Sensor A again experienced diminished adhesion post autoclave, but still yielded acceptable adhesion. Sensor B again detached cleanly, failing the test at 90 seconds.

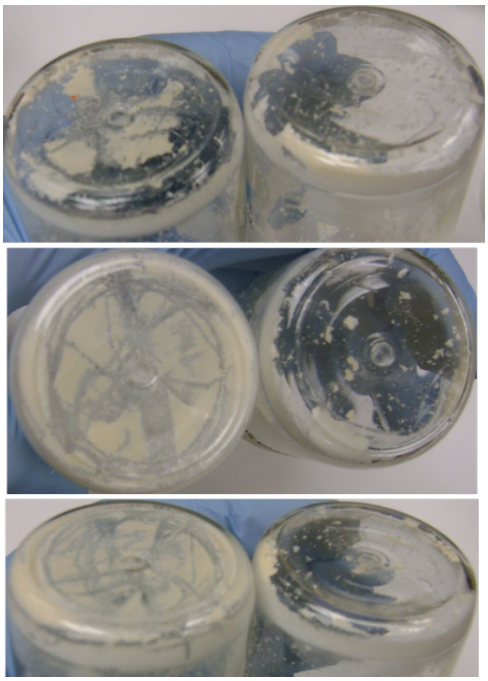

Figure 21: Pre-Autoclave Scrape Tested Bottle Bases of Sensor A versus Sensor B at Varying Plasma Treatment Times. We prepared bottles plasma treated at 60, 90, and 180 seconds and dispensed Sensor A or Sensor B into each. We scrape tested replicates of Sensor A bottles (left of all pictures) and Sensor B bottles (right of all pictures) for bottles plasma treated for 60 seconds (top), 90 seconds (middle), and 180 seconds (bottom).

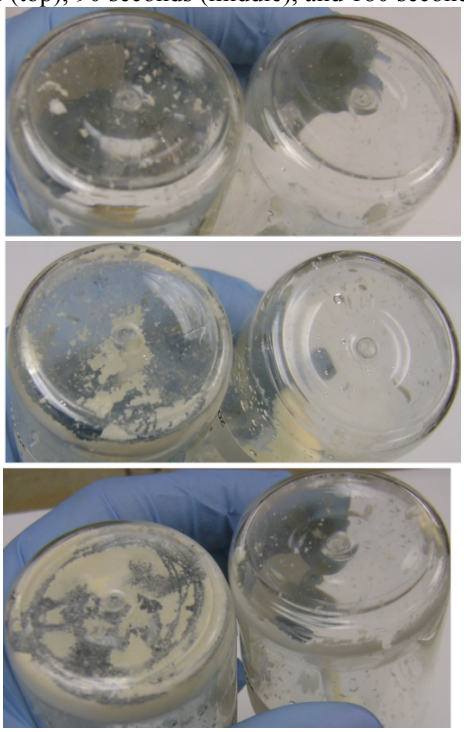

Figure 22: Post-Autoclave Scrape Tested Bottle Bases of Sensor A versus Sensor B at Varying Plasma Treatment Times. We prepared bottles plasma treated at 60, 90, and 180 seconds and dispensed Sensor A or Sensor B into each. After autoclaving the remaining un-scraped bottles, we scrape tested replicates of Sensor A bottles (left of all pictures) and Sensor B bottles (right of all pictures) for bottles plasma treated for 60 seconds (top), 90 seconds (middle), and 180 seconds (bottom).

Sensor B only yielded any sign of adhesion post-autoclave when treated for 180 seconds. This being said, 180 seconds of plasma treatment time is unfeasible for manufacturing. Even 90 seconds remains slightly too long for manufacturing, and thus we moved forward with a 60 seconds plasma treatment time.

Pilot Scale Evaluation

We assessed the adhesion levels of all four bottle conditions both pre- and post-autoclave. We found that only Sensor A dispensed into bottles plasma treated in Cayey yielded adhesion on the level of the current sensor in the glass bottle post autoclave (*Figure 23*). All other conditions failed.

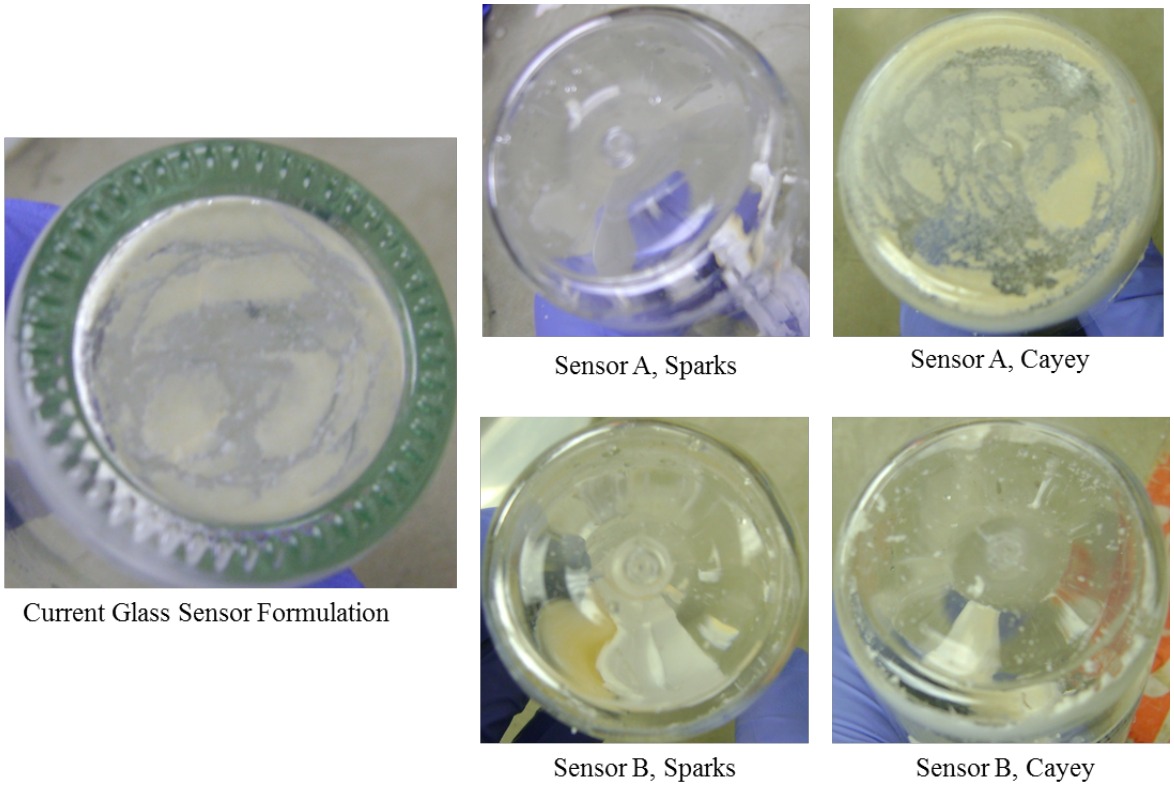

Figure 23: Scrape-Tested Bottle Bases from Post-Autoclave Pilot Samples. We scrape tested samples from each condition and compared the results to the current glass sensor (left). Sensor A in bottles plasma treated in Cayey, Puerto Rico (top right) passed the scrape test while Sensor B in bottles plasma treated in Cayey (bottom right) and Sensors A and B in bottles plasma treated in Sparks, MD (top left and bottom left, respectively) all failed the scrape test.

These results show not only that Sensor B does not adhere post-autoclave under any condition, but that the plasma treatments done in Sparks versus in Cayey yield different adhesion results.

We calculated the dynamic range of each bottle from the room air and nitrogen readings collected by the BACTEC 9240 (*Figure 24*). Sensor A plasma treated in Sparks and Cayey yielded averages of 200% and 204%, respectively. Sensor B yielded dynamic range averages of 296% and 310% for bottles treated in Sparks and Cayey, respectively. The current glass sensor, which we used as a control, yielded an average dynamic range of 340%.

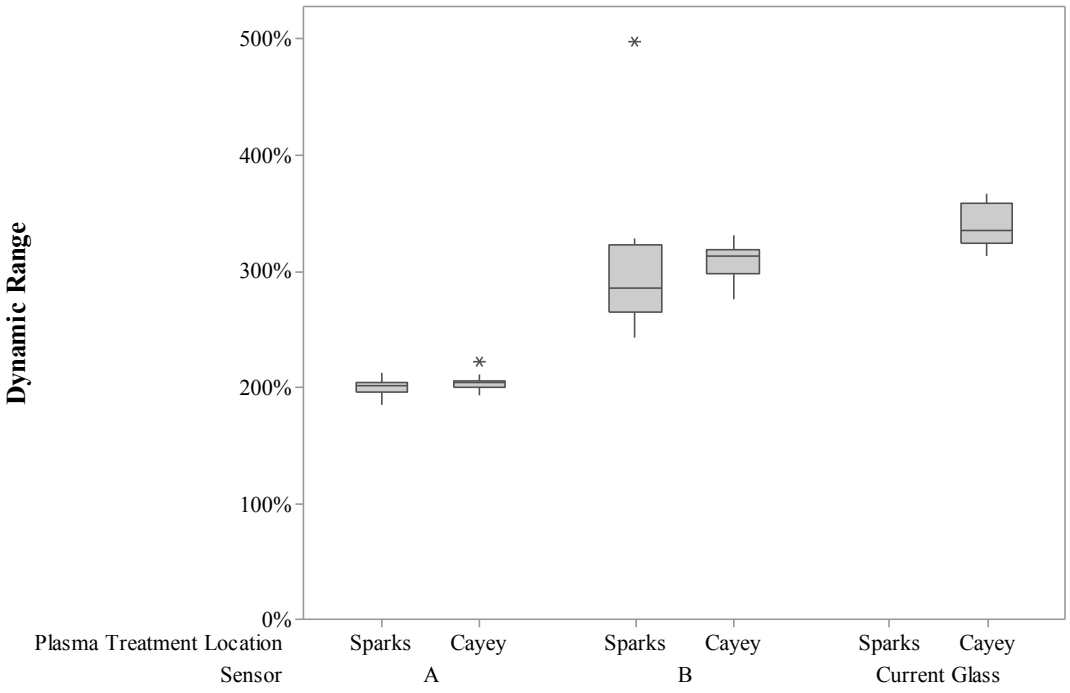

Figure 24: Boxplot of Dynamic Range of Voltage Signal for Each Condition of Pilot Scale Testing. We plotted the distribution of dynamic ranges across samples for each pilot scale condition. We used the current glass product for sale as a control These control bottles were prepared in Cayey, Puerto Rico and shipped to Sparks, MD where we performed dynamic range testing. For each distribution, outliers are noted by an asterisk (*).

Based upon these results, plasma treatment yields no significant effect on the dynamic range; however, an increased amount of adhesion promoter narrows the dynamic range. In order to

determine the cause for a smaller dynamic range, we looked specifically at the baseline and nitrogen readings of each sensor (*Figure 25*).

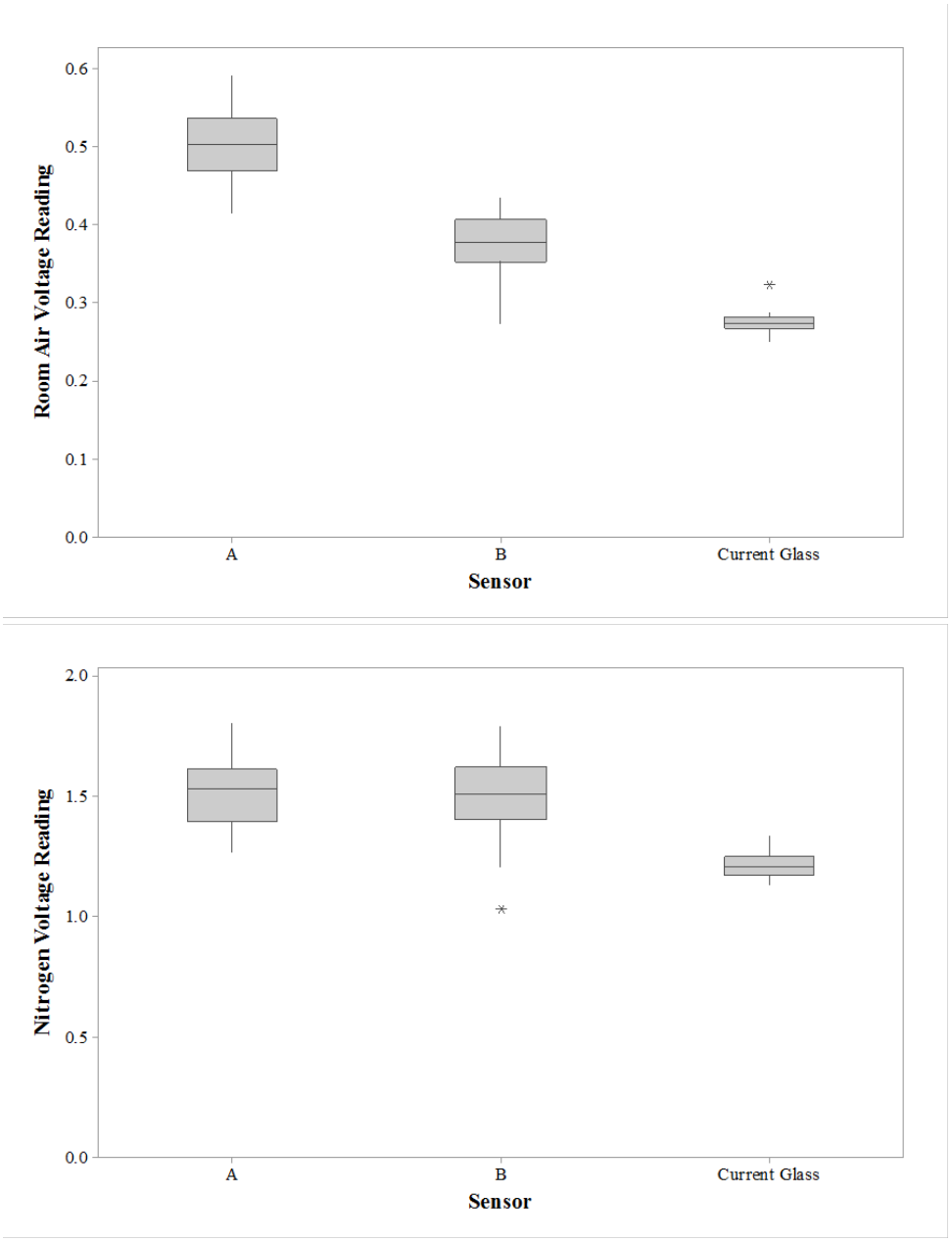

Figure 25: Boxplots of Room Air and Nitrogen Voltage Readings for Each Sensor of Pilot Scale Testing. Dynamic range results showed that variation in plasma treatment does not significantly affect the dynamic range across the same sensor. Thus, we plotted the distributions of room air readings (top) and nitrogen readings (bottom) across all Sensor A, Sensor B, and glass sensor samples. Outliers are denoted by an asterisk.

From these results, we saw that more adhesion promoter increases the baseline voltage reading of the sensor while leaving the nitrogen reading relatively unaffected. This indicates potential interference of the adhesion promoter with oxygen detection. Moreover, the higher baseline reading and narrower dynamic range of both warrant assessment of the effects on the sensitivity of growth detection by the sensor.

DISCUSSION

Conversion of the scrape test scale to one that calls a sensor as having acceptable or unacceptable adhesion allowed us to more clearly define parameters for sample preparation and select a formulation for further testing. Even with this, the scrape test remains inherently subjective, necessitating further investigation of methods to quantify and qualify sensor adhesion. While we did successfully select a sensor formulation and plasma treatment condition acceptable for scale-up, this formulation yielded a narrower dynamic range than the current glass product for sale. Furthermore, the results of the scrape test necessitated that we move forward only with Sensor A in bottles plasma treated in Cayey since the remaining conditions yielded unacceptable adhesion. Although further testing and scale-up will determine whether or not the narrower dynamic range affects sensor performance, results of the pilot testing warrant investigation of the cause of a higher baseline voltage reading and potential solutions for lowering it to yield a dynamic range on the order of the glass product.

Quantification of Adhesion

The scrape test is a highly qualitative, subjective method for assessing adhesion of a sensor to the BACTEC bottle. This made applying a quantitative scale to it very difficult, especially a scale with several levels. The difference between sensors that gave level 6 adhesion versus sensors that gave a level 9 adhesion proved minimal. Since both conditions yield adhesion throughout the

entire base of the bottle, both could be selected as a final product. Moreover, even a sensor yielding a level 3 adhesion could potentially be selected if it yields adhesion around the edges of the sensor, which would prevent culture material from seeping between the fluorescence indicator and detector. Defining adhesion levels on a binary scale allows for clearer definition of the formulations we should pursue for further testing by classifying them as acceptable or unacceptable. This eliminates any grey areas in placing sensors in one of four categories.

Calling a sample "acceptable" or "unacceptable" without a quantitative measurement remains subjective despite having references from current products. In order to accurately define adhesion levels that are acceptable and unacceptable, a quantitative measurement must be developed. From this, samples can be consistently tested for adhesion and confidently called as yielding acceptable or unacceptable adhesion. Due to the urgency and scope of this project, time did not permit development of a method; however, one suggestion for development includes defining a pull-up or scrape force limit that the sensor can tolerate before failing. Specifically, inverting the bottles and placing them in a swinging-bucket rotor centrifuge and increasing the speed until the sensor detached could serve as an accurate, efficient way to quantify the adhesion level of the sensor. While the swinging-bucket rotor may better simulate agitation of the blood culture bottle in a BACTEC, inverting the bottles in a fixed-angle rotor may serve better to define a force that the sensor can withstand. A method such as this would allow for more systematic development of all sensors of blood culture bottles.

Plasma Treatment Levels and Variations

For bottles plasma treated at the R&D site, increasing the length of treatment time noticeably increases the adhesion level of the sensor. While Sensor A showed increasing levels of adhesion across all lengths of time tested, Sensor B just barely started showing signs of adhesion

at the longest treatment time, 180 seconds. Thus, despite a positive correlation between plasma treatment time and adhesion, increasing treatment cannot fully make up for a smaller amount of adhesion promoter. For experimental purposes, one could continue to increase the plasma treatment time in order to determine the length of treatment time that yields the same adhesion levels as increased adhesion promoter i.e. Sensor A; however, longer plasma treatment times only increase manufacturing time. From a manufacturing standpoint, even 90 seconds would slow high throughput production, and thus a compromise between more adhesion promoter versus more plasma treatment must be made.

While increasing the length of time and holding the power of plasma treatment constant improves adhesion, stronger and longer plasma treatments may not be necessary. The power and length of plasma treatment at the manufacturing site (150W for 20s) was significantly lower and shorter than the power and length that we applied to bottles prepared at the R&D site (500W for 60s). The results of the pilot scale testing showed not only that Sensor A yields better adhesion than Sensor B, but that bottles plasma treated at the manufacturing site yield better adhesion than those treated at the R&D site. In terms of plasma treatment conditions, this suggests two possible explanations: (1) increasing the power of plasma treatment yields less favorable surface modification for adhesion; or (2) the equipment at the manufacturing site provides a more concentrated treatment, yielding increased surface modification and adhesion. While both explanations are possible, the second seems more likely based upon the conditions of the R&D plasma treatment instrument versus the manufacturing instrument. The plasma treatment instrument at the R&D site is a batch process. The instrument is very large and the samples take up less than 1/3 of the total volume inside the treatment chamber where the plasma is distributed more or less evenly throughout. The manufacturing site employs a continuous process, using an

assembly line apparatus that essentially applies the plasma treatment in a concentrated beam. This may provide a more even, direct surface modification for better adhesion.

It is critical to investigate the differences between plasma treatments we employ for development and plasma treatments applied in manufacturing. Defining these differences and developing a conversion factor to create equal conditions between development and manufacturing will minimize differences and unexpected adhesion issues experienced during scale-up. Moreover, if developmental processing conditions do not mimic manufacturing conditions, it becomes difficult to develop feasible solutions. Thus, it is important not only that the effect of plasma treatment is better understood, but that we are able to simulate manufacturing conditions for small scale R&D testing.

Pilot Scale Evaluation

Since proper sensor adhesion is required to avoid leakage of blood culture sample and interference with growth detection, the adhesion test essentially serves as a first line of assessment to eliminate any unacceptable formulations. As previously discussed, we found variation in adhesion for bottles treated at the manufacturing versus R&D sites. Thus, only Sensor A plasma treated in Cayey passed the adhesion test. We continued to characterize the signal ranges of every condition despite lack of feasibility of moving forward with Sensor B.

Quality testing on the current glass product does not include dynamic range testing. Thus, we included the glass bottle in all testing as a reference and found narrower dynamic range for all conditions. No significant variation in dynamic range across the same sensor with different plasma treatments indicates that surface modifications to the bottle have no effect on dynamic range;

however, adding and increasing the amount of adhesion promoter increased the baseline reading and effectively narrowed the dynamic range.

The detailed chemical mechanisms of the sensor are beyond the scope of this project. This being said, a higher room air reading and constant nitrogen reading of a sensor that detects diminishing oxygen levels suggests that the adhesion promoter interferes with the detection of oxygen. Testing a formulation with a similar adhesion promoter with less functional groups than the current promoter in development may prevent this interference and increase the dynamic range. Yet while a smaller dynamic range may suggest a lower sensitivity to oxygen depletion and thus bacterial growth, further biological testing must be done in order to determine if it does in fact affect sensor performance.

CONCLUSIONS AND RECOMMENDATIONS

For conversion of fluorescence-based sensors from glass to polycarbonate bottles, increasing the amount of adhesion promoter in the formulation and applying short, concentrated plasma treatment to the bottles provides the sensor with even adhesion to the bottle base. In order to yield acceptable adhesion however, the detection signal readings become compromised as more adhesion promoter narrows the dynamic range. Unknowns relative to the amount of necessary sensor adhesion to prevent sensor displacement, as well as the effects of narrowed dynamic range on detection sensitivity, make it difficult to optimize conditions for conversion to plastic bottles.

A quantitative measurement of sensor adhesion would allow for definition of standards for what qualifies a formulation as yielding acceptable versus unacceptable attachment. Generally speaking, quantifying the force necessary to detach the sensor from the bottle allows establishment of thresholds and characterization of formulation adhesion. Centrifuging inverted bottles or applying a force gauge to pull up the sensors are simple, cost-effective solutions for this

quantification. With a method and standards in place, determining the effects of differing levels of adhesion promoter and plasma treatment becomes easier and allows for more strategic development of formulations.

Once sensor attachment standards are established, alterations to formulations must focus on signal detection. We saw that increased adhesion promoter yielded a higher baseline signal and narrowed the dynamic range, but whether or not this will negatively impact detection sensitivity remains unknown. It is recommended not only that scaled up biological testing on the Sensor A formulation is performed, but also that further investigation occurs to determine why increased adhesion promoter increases the baseline reading. Additionally, formulation development using alternative adhesion promoters with less functional groups may improve sensor attachment without decreasing the dynamic range. With a better understanding of the attachment and dynamic range levels necessary for accurate growth detection, full conversion from glass to plastic bottles can be made. This will allow for easier transport and disposal of BACTEC blood culture bottles, ultimately decreasing the cost and time required for employing the diagnostic workflow for blood stream infections.

APPENDIX 1: ADDITIONAL FIGURES AND TABLES

Table A1.1: Microorganisms Tested in Baseline Study.

TYPE	ID	CHARACTERISTICS
Gram Negative	*Acinetobacter baumannii*	wild type
Gram Negative	*Acinetobacter baumannii*	Multidrug-resistant (MDR), OXA-23 β-lactamase, NDM-β-lactamase-1-producing (NDM)
Gram Negative	*Enterobacter cloacae*	wild type
Gram Negative	*Enterobacter cloacae*	high-level cAmpC
Gram Negative	*Escherichia coli*	wild type
Gram Negative	*Escherichia coli*	Original-spectrum β-lactamase (ESBL)-producing
Gram Negative	*Escherichia coli*	NDM, aminoglycoside resistant
Gram Negative	*Klebsiella pneumoniae*	wild type
Gram Negative	*Klebsiella pneumoniae*	extended-spectrum β-lactamase (ESBL)-producing
Gram Negative	*Klebsiella pneumoniae*	Klebsiella pneumoniae carbapenemase (KPC)-producing
Gram Negative	*Pseudomonas aeruginosa*	wild type
Gram Negative	*Pseudomonas aeruginosa*	MDR, VIM-2-producing
Gram Negative	*Proteus mirabilis*	wild type
Gram Negative	*Proteus mirabilis*	ESBL
Gram Negative	*Serratia marcescens*	wild type
Gram Negative	*Serratia marcescens*	SME-1-producing

Gram Positive	*Enterococcus faecalis*	Vancomycin resistant Enterococci (VRE) (vanB)
Gram Positive	*Enterococcus faecalis*	wild type
Gram Positive	*Enterococcus faecium*	wild type
Gram Positive	*Enterococcus faecium*	VRE
Gram Positive	*Staphylococcus aureus*	wild type, NCF pos
Gram Positive	*Staphylococcus aureus*	Methicillin-resistant Staphylococcus aureus (MRSA)
Gram Positive	*Staphylococcus aureus*	wild type, NCF neg, pen S
Gram Positive	*Staphylococcus aureus*	MRSA
Gram Positive	*Staphylococcus epidermidis*	wild type
Gram Positive	*Staphylococcus epidermidis*	Tetracycline resistant
Gram Positive	*Staphylococcus lugdunensis*	Clindamycin and erythromycin resistant
Gram Positive	*Staphylococcus saprophyticus*	Oxacillin and penicillin resistant
Streptococcus	*Streptococcus pneumoniae*	resistant
Streptococcus	*Streptococcus pneumoniae*	Penicillin resistant

Table A1.2: Dilution Scheme for Plating PBCs and Output Tubes.

Sample Number	Procedure	Dilution Factor from Original Sample	Amount Plated	Expected CFU/mL in Original Sample if Plate is Readable [multiplier]
1	210µL output tube or PBC into 20mL saline	10^{-2}		
2	210µL sample 1 into 10mL saline	10^{-4}	40µL sample 2	$1.5x10^{7}$ [250,000]
3	560µL sample 2 into 5mL saline	10^{-5}	40µL sample 3	$1.5x10^{8}$ [2,500,000]
4	560µL sample 3 into 5mL saline	10^{-6}	40µL sample 4	$1.5x10^{9}$ [25,000,000]
5	560µL sample 4 into 5mL saline	10^{-8}	40µL sample 5	$1.5x10^{10}$ [250,000,000]

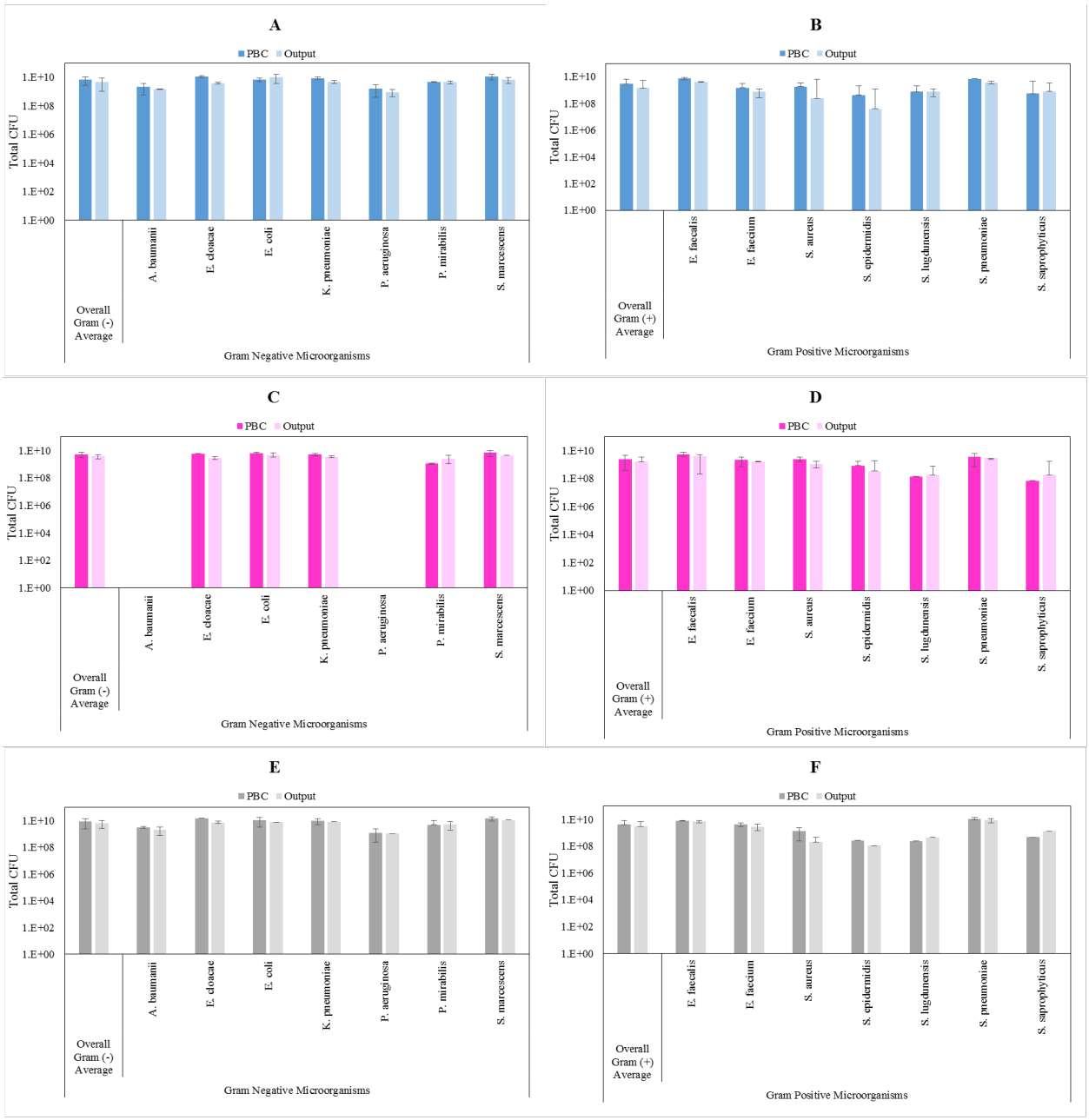

Figure A1.1: Total CFU in Original PBC versus Output for Each Microorganism and Media Type Tested in the Baseline Study. We averaged the PBC and output plate counts across the strains of each microorganism for each type of media, and then used these counts to calculate the percent recovery of bacteria from filtration. (A-B) Standard Aerobic Media. (C-D) Lytic Anaerobic Media. (Note: BACTEC detected no growth for *A. baumanii* and *P. aeruginosa* in Lytic Anaerobic media due to their aerobic nature). (E-F) PLUS Aerobic Media.

APPENDIX 2: SAMPLE CALCULATIONS

Sample Calculation for Dynamic Range of Fluorescence-Based Oxygen Sensor

After performing the dynamic range protocol, the mean signal readings after stabilization at room air exposure and stabilization at zero-oxygen levels (nitrogen gas purge) can be collected for each bottle. The room air reading serves as the baseline signal level and accounts for any signal noise, while the nitrogen purge reading serves as the maximum signal level. The dynamic range is calculated by substituting these values into Equation 1 to yield:

$$\text{Dynamic Range} = \frac{\text{(Nitrogen Voltage)-(Room Air Voltage)}}{\text{Nitrogen Voltage}} \times 100\% \qquad \text{[Equation 2]}$$

If the stabilized room air reading is measured as 0.268V and the stabilized nitrogen purge reading is measured as 1.135V, the dynamic range can be calculated as follows:

$$\text{Dynamic Range} = \frac{1.135-0.268}{0.268} \times 100\% = 324\% \qquad \text{[Equation 3]}$$

This calculation was performed for each sensor, and the average dynamic range was then calculated for each condition, or sensor formulation.

LITERATURE CITED

1. Singer M, Deutschman CS, Seymour CW, Shankar-Hari M, Annane D, Bauer M, Bellomo R, Bernard GR, Chiche J, Coopersmith CM, et al. 2016. The third international consensus definitions for sepsis and septic shock (sepsis-3). Jama 315(8):801-10.

2. Torio CM and Andrews RM. 2013. National inpatient hospital costs: The most expensive conditions by payer, 2011: Statistical brief #160. Healthcare Cost and Utilization Project (HCUP) Statistical Briefs [Internet] .

3. Fleischmann C, Scherag A, Adhikari NKJ, Hartog CS, Tsaganos T, Schlattmann P, Angus DC, Reinhart K. 2016. Assessment of global incidence and mortality of hospital-treated sepsis. current estimates and limitations. Am J Respir Crit Care Med 193(3):259-72.

4. Angus DC and van dP. 2013. Severe sepsis and septic shock. N Engl J Med 369(9):840-51.

5. Gauer RL. 2013. Early recognition and management of sepsis in adults: The first six hours. Am Fam Physician 88(1):44-53.

6. Center for Devices and Radiological Health. 2009. Guidelines on review criteria for assessment of antimicrobial susceptibility devices. U.S. Department of Health and Human Services, Food and Drug Administration, Rockville, MD.

7. Singhal N, Kumar M, Kanaujia PK, Virdi JS. 2015. MALDI-TOF mass spectrometry: An emerging technology for microbial identification and diagnosis. Frontiers in Microbiology 6:791.

8. Murray PR. 2012. What is new in clinical Microbiology—Microbial identification by MALDI-TOF mass spectrometry: A paper from the 2011 william beaumont hospital symposium on molecular pathology. The Journal of Molecular Diagnostics : JMD 14(5):419-23.

9. van Veen SQ, Claas EC, Kuijper EJ. 2010. High-throughput identification of bacteria and yeast by matrix-assisted laser desorption ionization-time of flight mass spectrometry in conventional medical microbiology laboratories. J Clin Microbiol 48(3):900-7.

10. MALDI-TOF: Schematic and Theory of MALDI [Internet]; c2015 [cited 2018 Jun 26,]. Available at:

    https://chem.libretexts.org/Textbook_Maps/Analytical_Chemistry/Supplemental_Modules_(Analytical_Chemistry)/Instrumental_Analysis/Mass_Spectrometry/MALDI-TOF#Schematic_and_Theory_of_MALDI

11. Phoenix Gram Positive Laboratory Procedure [Internet] [cited 2018 Jun 6,]. Available from : http://legacy.bd.com/ds/technicalCenter/clsi/clsi-Phoenix_GramPositive_V5.15_V4.31.pdf .

12. MALDI biotyper bacterial test standard. 2015. Billerica, MA: Bruker Daltonics, Inc.

13. Bruker Daltonics US IVD Bacterial Test Standard Instructions for Use. Entire protocol available online at:

    https://www.bruker.com/fileadmin/user_upload/8-PDF-Docs/Separations_MassSpectrometry/InstructionForUse/IFU_604537_US_IVD_BTS_Revision_C.pdf

14. Ando T, et al. 2012. Simulation of fouling and backwash dynamics in dead-end microfiltration: Effect of pore size. Journal of Membrane Science 392-393:48-57.

15. Davis RH. 1992. Modeling of fouling of crossflow microfiltration membranes. Sep Purif Methods 21(2):75-126.

16. Alatoom AA, Cunningham SA, Ihde SM, Mandrekar J, Patel R. 2011. Comparison of direct colony method versus extraction method for identification of gram-positive cocci by use of bruker biotyper matrix-assisted laser desorption Ionization–Time of flight mass spectrometry. J Clin Microbiol 49(8):2868-73.

17. Schulthess B, Brodner K, Bloemberg GV, Zbinden R, Böttger E,C., Hombach M. 2013. Identification of gram-positive cocci by use of matrix-assisted laser desorption

Ionization–Time of flight mass spectrometry: Comparison of different preparation methods and implementation of a practical algorithm for routine diagnostics. J Clin Microbiol 51(6):1834-40.

18. Plastic Collection Tubes Decrease Risk of Employee Injury [Internet] [cited 2018 Jul 2,]. Available from : https://www.bd.com/en-us/offerings/capabilities/specimen-collection/educational-services-and-materials/labnotes/labnotes-13-2-2003 .

19. U.S. Department of Health and Human Services, Food and Drug Administration. 2016. Pre-market clearance 510(k) BD BACTEC™ Plus Aerobic/F. https://www.accessdata.fda.gov/ cdrh_docs/pdf11/K113558.pdf.

20. U.S. Department of Health and Human Services, Food and Drug Administration. 2016. Pre-market clearance 510(k) BD BACTEC™ Plus Anaerobic/F. https://www.accessdata.fda.gov/ cdrh_docs/pdf14/K141810.pdf.

21. U.S. Department of Health and Human Services, Food and Drug Administration. 2016. Pre-market clearance 510(k) BD BACTEC™ Peds PlusTM/F. http://www.accessdata.fda.gov/cdrh_docs/pdf15/K151866.pdf.

22. van Griethuysen AJ, Jansz AR, Buiting AG. Comparison of fluorescent BACTEC 9000 MB system, septi-chek AFB system, and lowenstein-jensen medium for detection of mycobacteria. J Clin Microbiol 1996 October 01;34(10):2391-4.

23. BMS DIAGNOSTICS (M) SDN BHD. 2014. Fluorescent technology in the BD BACTEC™ automated blood culture system. http://www.bmsd.com.my/files/editor_files/file/July-2014.pdf

24. Cui L, Ranade AN, Matos MA, Dubois G, Dauskardt RH. 2013. Improved adhesion of dense silica coatings on polymers by atmospheric plasma pretreatment. ACS Appl Mater Interfaces 5(17):8495-504.

25. What is surface treatment? [Internet]; ca [cited 2018 Jul 2,]. Available from: https://tantec.com/what-is-surface-treatment.html .

26. The basics of plasma treatment [Internet]; cb [cited 2018 Jul 2,]. Available from: https://tantec.com/the-basics-of-plasma-treatment.html .

Curriculum Vitae

SHANNON E. MARTELLO
7 Stablers Court, Parkton, MD 21120
MartelloShannon@gmail.com, (443) 909-0276

EDUCATION

Johns Hopkins University **Baltimore, MD** **July 2018**
Master of Science in Engineering, Chemical and Biomolecular Engineering
GPA: 3.7

Johns Hopkins University **Baltimore, MD** **May 2017**
Bachelor of Science, Chemical and Biomolecular Engineering
Concentration: Molecular and Cellular Bioengineering
GPA: 3.1 (Dean's List: Fall 2016—Spring 2017)

EXPERIENCE

Becton Dickinson Diagnostic Systems Sparks, MD **January 2018 – July 2018**
Microbiology Engineering Co-Op

- Designed, executed, and troubleshot experiments in order to provide baseline performance data of a filtration system that isolates bacteria from a blood culture to allow for more rapid diagnosis and treatment of a bloodstream infection
- Conducted early-stage technical development research for the development of a next-generation fluorescence-based sensor for an automated culture system intended for clinical microbiology labs
- Evaluated prototypes with members of a cross-functional product development team for a product line extension expected to launch in 2020
- Prepared bench- and pilot-scale research formulations to assess compatibility and performance with instrumentation currently on the market and in development

Biodesix, Inc. **Boulder, CO** **May 2017 – August 2017**
Assay Development Intern

- Led data analysis of over a year and a half of QC metrics from the CLIA lab in order to provide the team with relevant quality standards to monitor the performance of on-market RNA-based assays
- Executed and documented experiments to support the development of a new DNA-based assay for the KRAS gene mutation
- Executed and documented verification experiments for a new RNA-stabilization formulation in the blood collection tube

Tulkoff Food Products **Baltimore, MD** **May 2016 – August 2016**
Product Development Intern

- Tested experimental product batches for viscosity, brix, pH, and density
- Analyzed original products and conducted QC tests in order to remove high fructose corn syrup from Tulkoff's emulsion products
- Consulted with companies and analyzed their products to develop items that better suit needs

TECHNICAL SKILLS

- Minitab, MATLAB, Simulink, Aspen Plus, Arduino, SQL, PyMOL, QuantaSoft, DOE, Microsoft Office (Word, PowerPoint, Excel, Outlook)
- UV-VIS, FTIR, MALDI-ToF MS, Cell Culture, Optical Microscopy, Microfiltration, Tangential Flow Filtration, Droplet Digital PCR, DNA and RNA Extraction, Antimicrobial Susceptibility Testing, Centrifugation, Bioreactor Operation